Case Studies on Transport Policy 12 (2023) 100972

Contents lists available at ScienceDirect

Case Studies on Transport Policy

journal homepage: www.elsevier.com/locate/cstp

The fluvial passenger transport design problem with an electric boat

Camilo Vélez *, Alejandro Montoya

Departamento de Ingeniería de Producción, Universidad EAFIT, Carrera 49 No 7 Sur-50, Medellín, Colombia

ARTICLE INFO

Keywords:
Electric boat
Fluvial transport operation
Photovoltaic charging stations

ABSTRACT

In this paper, we introduce a new optimization problem called the fluvial passenger transport design problem with an electric boat (FPTDP-EB). This problem is inspired by a future fluvial operation using electric boats (EBs) for passenger transportation between two cities on the banks of the Magdalena River in Colombia. The FPTDP-EB consists of selecting the battery capacity for the EB, the charging infrastructure to install, and the scheduling of each round trip. For the charging infrastructure, we considered the location of the charging stations, their charging powers, and whether they would have photovoltaic (PV) components. For stations with PV components, we also considered the number of PV panels and the capacity of their energy storage systems. For this problem, we considered the stochastic behavior of solar irradiance, the arrival times of candidate passengers for the EB, and power outages for the electric grid. The objective function is to minimize the operation's investment cost, the maintenance cost of the charging stations and the cost of the energy to be purchased from the grid during a time horizon. We propose a branch-and-bound algorithm with a Monte Carlo simulation to solve the FPTDP-EB. The latter evaluates the feasibility of each solution and estimates the amount of energy to be purchased from the grid during the time horizon. Our method solves the operation design for the Magdalena River scenario in reasonable computation times for a strategic problem. Additionally, we perform some sensitivity analyses to evaluate how certain factors, such as the energy density of batteries, could impact the structure of the solution. Our results show that the use of photovoltaic charging stations helps minimizing the overall cost of the operation, and makes it more resilient towards power outages. Additionally, as the energy density of electric batteries continues improving, the overall cost of these type of operations is expected to decrease significantly.

1. Introduction

Governments and companies have recently been concerned about pollution and the dependence of the transportation sector on fossil fuels (Umar et al., 2021). Electric vehicles (EVs) have risen to reduce such dependence as they do not emit greenhouse gases during their operation (International Energy Agency, 2021). However, EVs have some technical limitations compared with internal combustion vehicles (ICVs). These include their lower driving autonomy, lengthy recharging times, and expensive batteries. These batteries may even be up to 30% of the total cost of an electric car (Bloomberg, 2019). Because of these limitations, transport operations using EVs require some special planning to be technically and economically feasible.

Most electric mobility applications have been implemented in urban areas because of the autonomy limitations of these vehicles. Additionally, urban areas tend to have more reliable electric power grids than rural areas (Krupp, 2010), which is crucial for charging EVs. Nonetheless, rural transportation must not be ignored, as it is essential for providing access to employment and public facilities, thus increasing the well-being for rural communities (U.S. Department of Transportation, 2019), and for supporting a country's overall transport system, as for example 68% of all lane-miles in the United States are in rural areas (U.S. Department of Transportation, 2022). Therefore, rural electric transportation is also an interesting research topic. Concerning the autonomy of EVs, recent developments in electric batteries have increased their energy density (Cao et al., 2020). This means that batteries can store more energy per unit of mass, increasing the driving range of EVs. One solution to the reliability issues of electric grids in rural areas is the use of photovoltaic charging stations (PVCSs). Such stations may use photovoltaic (PV) energy and energy from the electric grid to charge EVs (Shepero et al., 2020).

One type of rural transportation that has not been as commonly researched as land transport, but that is essential nonetheless, is the fluvial one. Fluvial transport operations are especially crucial in areas

* Corresponding author.
E-mail addresses: cvelezg10@eafit.edu.co (C. Vélez), jmonto36@eafit.edu.co (A. Montoya).

https://doi.org/10.1016/j.cstp.2023.100972
Received 10 August 2022; Received in revised form 23 February 2023; Accepted 27 February 2023
Available online 3 March 2023

such as the Ecuadorian Amazonía, where boats account for 90% of the region's transportation (Jaimurzina et al., 2017). Electric boats (EBs) are interesting vehicles for these fluvial operations as they pollute both air and water less than internal combustion boats (ICBs) do. Additionally, gasoline may be up to four times more expensive in some rural areas than in urban settings, which increases the operational costs for ICBs (Alvarado Ponce, 2017). Some initiatives have implemented electric fluvial transportation in Latin America. Jaimurzina et al. (2017) assessed some fluvial routes of up to 60 km using EBs to transport children to their schools across the Putumayo River. Project Kara Solar implemented a solar-powered EB to transport indigenous people in up to nine communities across 67 km in Ecuador (UNEF, 2017).

Following such initiatives, the alliance "ENERGETICA 2030" (Energetica 2030, 2022) aims to implement an electric fluvial transport operation using EBs in Magangué, Colombia. Such location was selected as it is a port in the Magdalena River (Colombia's principal river) connecting multiple neighboring areas. Of all the fluvial operations departing from Magangué's port, the project selected a round trip between the former and the municipality of Pinillos for a total route length of about 110 km. For the remainder of this research, we refer to a back and forth journey between Magangué and Pinillos as a round trip, whereas the individual routes Magangué-Pinillos or Pinillos–Magangué are simply referred to as trips (the outward and return ones, respectively). Fig. 1 shows a representation of these trips. ICBs perform such fluvial transport operations for passenger transportation at the time of this writing. This project aims to perform this fluvial transport operation using an EB charged using PVCS or standard charging stations (SCSs), which are entirely supplied from the electric grid.

This operation must first be designed accounting for the technical considerations of the EB to perform this transport operation using an EB. To do so, we solve an optimization problem to determine the required infrastructure for the operation and scheduling of each round trip. The infrastructure decisions consist of selecting the capacity of the battery to

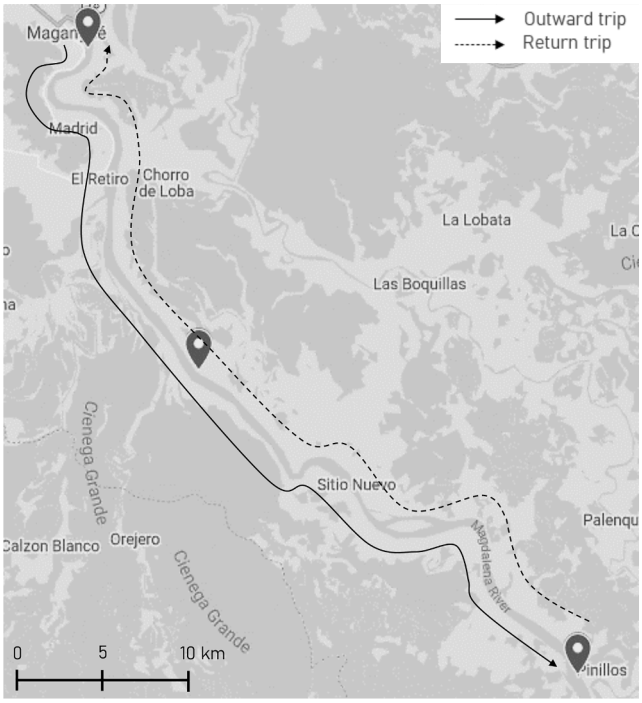

Fig. 1. Fluvial route selected by ENERGETICA 2030.

be installed in the EB and the charging infrastructure to be installed. This last decision includes the station locations at candidate nodes along the riverbank, the charging power of each station, and whether a station will be a SCS or a PVCS. For the latter, the number of PV panels and the capacity of its energy storage system (ESS)[1] must also be selected. We note that the technical design of the components for the EB and the stations is out of the scope of our research, we select which assets to install from commercially available ones. The scheduling decisions include the average speeds of the EB during the outward and return trips individually and the daily number of round trips and their departure times from Magangué. In making decisions, we consider the stochastic behavior of solar irradiance, the time between the arrivals of candidate passengers at each port, and the possibility of having power outages at each station. The objective function is to minimize the sum of the investment costs, the maintenance cost of the charging stations and the cost of the energy to be purchased from the electric grid for the EB to operate during a given number of years. The maintenance cost of the EB is not accounted for as the problem only selects its battery capacity. We named this problem the fluvial passenger transport design problem with an electric boat (FPTDP-EB). Even though this research focuses on the case study of ENERGETICA 2030 in Magangué, the FPTDP-EB is applicable to other electric fluvial transport operations.

We propose a two-stage simulation-based branch-and-bound algorithm to solve the FPTDP-EB. The first stage is an integer problem that determines the infrastructure and scheduling decisions using a branch-and-bound algorithm. This stage also calculates the investment costs for the infrastructure plus the maintenance cost of the charging stations. The second stage evaluates the operation of the EB during a given number of years assessing the feasibility of each solution and estimating the cost of energy to purchase from the grid through a Monte Carlo simulation. Using this approach, we solved the FPTDP-EB for the case study of ENERGETICA 2030 in reasonable computation times for a strategic problem. The approach implicitly evaluates all possible solutions of the problem accounting for the stochastic variables. As this method finds the best solution for the operation design, it is not necessary to implement a mathematical formulation as other works in the literature about infrastructure estimation for EBs have done. Additionally, we run different sensitivity analyses with varying numbers of days feasible for the simulation, energy densities of the EB's battery, and average times between outages and their average duration and evaluate a scenario with low solar irradiance.

The main contributions of this paper are fourfold; (i) this is a research around electric fluvial transportation, a type of transportation that is crucial in certain regions of the world, but that has not been as widely researched as electric land transportation; (ii) we propose a new optimization problem that includes relevant components for fluvial transport operations with EBs, which, to the best of our knowledge, have not been included in similar strategic problems in the literature. These components consists of: dealing with multiple trips, selecting the speeds and departure schedule of the EB, facing the stochastic nature of solar irradiance, considering power outages and handling a stochastic number of passengers; (iii) we propose a two-stage simulation-based branch-and-bound algorithm that is able to solve real-world instances of the optimization problem, such as the one from our case study; and (iv) we evaluate multiple scenarios for the operation of the EB in our computational experiments to assess the impact that the PVCSs (and therefore the solar irradiance), the expected improvements in battery energy densities, the required reliability of the operation and the power outages have in the solution of the problem.

The remainder of this paper is organized as follows. Section 2 presents a literature review of electric battery sizing, charging stations sitting and sizing, and optimization research on EBs. Section 3 describes some technical aspects of the operations of EBs and PVCSs. Section 4 formally introduces the FPTDP-EB. Section 5 describes the solution approach consisting of the simulation-based branch-and-bound algorithm. Section 6 presents the case study and the computational-

[1] An ESS is a PVCS's own battery, usually used to store its own PV generation

experiments. Sections 7 presents some insights that may help future implementations of electric fluvial transport operations. Finally, Section 8 concludes the paper.

2. Literature review

Because the novelty of the FPTDP-EB is the application of electric mobility in fluvial transport operations, the following literature review is focused on topics regarding electric mobility. We divided this literature review into two sections. Section 2.1 presents a general picture of the current adoption of EVs, addressing which types of EVs have been more widely adopted than others. Section 2.2 reviews the literature related to specific topics of the FPTDP-EB. For doing so, we first reviewed the literature related to the energy storage capacity for EVs and the location of stations. This is because they are two of the main decisions of the FPTDP-EB. We then examined optimization problems in fluvial operations.

2.1. General picture of the adoption of EVs

The global market of EVs has been constantly increasing with the years, with a 41% increment from 2019 to 2020 (International Energy Agency, 2021). This behavior has been promoted by the private and public sectors alike. Certain companies have made a considerable commitment to implement EVs in their operations, such as for example Amazon which ordered a fleet of 100.000 electric vans that would be operating by 2030 (Insider, 2021). On the other hand, governments tend to focus on adapting the electric infrastructure for the EVs and passing policies to endorse their use. On that topic, Chen et al. (2020) reviewed the efforts that the United Kingdom is performing towards the adoption of EVs. The authors concluded that while the UK's strategy of improving battery technologies and the charging infrastructure will increase the adoption of EVs, some challenges will arise in topics related to the electric grid and the users of the EVs (with costs, for example). There are also some areas where the public and private sectors cooperate, such as the installation of charging stations. China for example had 1.68 million stations by the end of 2020, with little over half of them being owned by private companies (Bloomberg, 2021).

Land vehicles have had the most widespread adoption among the different types of EVs. Apart from electric cars which are the most representative, electric buses for example are getting significant endorsements from local governments. For instance some cities in USA, England or Mexico have passed laws to only purchase electric buses from 2025 onwards (Pelletier et al., 2019). The market of electric two-wheelers (motorcycles and bicycles) has also been thriving, specially on Asia (Eccarius and Lu, 2020). For example, in 2020 there were 33.9 million electric two-wheelers produced in China alone, representing around 30% of the total number of two-wheelers produced in the country that year (Research and Markets, 2021). On the other hand, the adoption of vehicles such as EBs and electric airplanes is still limited (Campillo et al., 2019; Guardian, 2020). In that regard, in 2021 EBs accounted for only about 2% of the total market of EVs (Foresights, 2021). However, as previously mentioned there have been some implementations of electric fluvial transport operations in Latin America for example, such as that of Jaimurzina et al. (2017) or project Kara Solar (UNEF, 2017). To minimize the cost of this type of operations, optimization models are needed. Because of that, the following section reviews some optimization problems from the literature which studied certain topics related to the FPTDP-EB.

2.2. FPTDP-EB related literature

In estimating the energy storage capacity for EVs, some works consider sizing hybrid ESSs consisting of batteries and ultracapacitors, whereas some others sized only electric batteries. For this literature review, we considered works that used either of the aforementioned alternatives. Aiming to minimize the investment costs, Ostadi and Kazerani (2014) used a particle swarm optimization algorithm to size a hybrid ESS for installation in an electric bus. They evaluated their solutions using a given driving profile. Considering both the investment and degradation costs, Song et al. (2014) used a multiobjective genetic algorithm to size another hybrid ESS for an electric bus. They assessed the effects of different sizes of the hybrid ESSs in terms of their degradation. Another work considering both investment and degradation costs is that of Zhang et al. (2017a). Additionally, the authors also considered the cost related to the weight of the hybrid ESS. They used a nondominated sorting genetic algorithm to optimize the three objectives via multiple Pareto-optimal solutions. Unlike the authors of the mentioned previous works, Baek et al. (2020) performed their battery sizing on the basis of the revenue from the operation of an EV. They determined the optimal battery size for an electric truck given the number of deliveries its battery allowed it to perform for a set of simulated days. Their algorithm iterated over a set of battery sizes, estimating for each one the profit given by the revenue of the deliveries minus the estimated battery degradation cost and the cost of energy required to fully recharge the truck between days.

The location of charging stations has been heavily studied in the past couple of years because of the rise of electric mobility. Recently, Galadima et al. (2019) did a review considering SCSs, PVCSs, and wind-powered stations. They divided their reviewed literature into works that considered the problem from the point of view of a transportation system, an electricity network, and a hybrid of both. We focused our literature review only on the first type of problems. The topic of locating SCSs has been deeply researched. Sun et al. (2018) used a mixed-integer program (MIP) formulation to locate SCSs while also deciding their charging power, akin to what we do in the FPTDP-EB. Their objective function was to maximize the coverage and supplied demand of EVs with a limited budget. In locating PVCSs, Quddus et al. (2019) studied the problem from a strategic and operational perspective, as in the FPTDP-EB, as they considered both investment and operative costs. They minimized both the investment cost in PVCSs and the costs of charging EVs using a hybrid method of the sample average approximation and progressive hedging algorithm. They considered that the investment could be split into multiple simulated years depending on the flow of EVs, with each year having different associated costs. An additional infrastructure decision that can be made when installing PVCSs is sizing their components, such as PV panels and ESS, as in the FPTDP-EB. For this topic, Yan and Ma (2020) used a convex programming model to meet the stochastic demand of EVs in a PVCS from both an infrastructure and operative perspective. They considered the arrival time, initial energy level, and number of EVs that could be potential clients of the PVCS as stochastic variables. Their objective function was to minimize the summed costs of installing PV panels, ESS, charging powers, and the transformer and the energy to be purchased from the grid minus the revenue of charging EVs.

As previously mentioned, there is not much research in optimization problems regarding electric fluvial mobility. To our best knowledge, Zhang et al. (2017b) were the first authors to consider the location of SCSs for EBs. They used a MIP formulation to perform a two-staged optimization to determine first the location and then the service capacity of some SCSs to supply a given demand of EBs. Even though not an operational design problem, another optimization work regarding electric fluvial mobility is that of Villa et al. (2019). They determined the optimal speeds and charging decisions of an EB during a fixed route via a mixed-integer linear programming (MILP) formulation. Their objective function was to minimize the energy to be purchased from the grid and the EB's battery degradation. Both previous works considered only SCSs. Using PVCSs, Lukuyu et al. (2020) minimized the number of stations required to meet a certain demand of EBs while also meeting an additional energy demand from household activities for a case study in Lake Victoria. The authors used an iterative algorithm and a Monte Carlo simulation to simulate a year's worth of the system's operation. They

considered routes that, at the time of this writing, are being performed by ICBs to estimate the energy demand for EBs. However, they did not evaluate en-route charging operations. To the best of our knowledge, the most similar works to our current research are those of Villa et al. (2020) and Vélez et al. (2020), as both considered en-route charging operations. The first work used a MILP formulation to determine the battery capacity of an EB and the location of off-grid PVCSs. Their objective was to minimize the investment costs. The second work used a constructive heuristic to face a similar problem while also deciding on the sizing of the PVCSs' components. Unlike the present research, both of the previous works consider only one trip for the EB with a predefined maximum route time, solar irradiance as a fixed deterministic profile, and the number of passengers and the speed of the EB as constants.

A summary of the different components that strategic optimization problems with EBs in the literature have considered is shown in Table 1. It can been seen that, to our best knowledge, the works that make infrastructure decisions for EBs have not considered decisions regarding the scheduling of their operations. We consider that accounting for the latter type of decisions allows the infrastructure to meet the requirements of the operation more precisely so that the investment is not underestimated or overestimated. Furthermore, we evaluate the trade-off between investing in PV systems and buying energy from the grid. This evaluation needs the scheduling of the EB to be known to determine the amount of required energy from either source. Apart from making both infrastructure and scheduling decisions, we consider the dynamic behavior of solar irradiance for PV generation and random variables such as the arrival time of passengers and the possibility of having power outages.

3. Technical aspects

This section provides a short explanation of some technical aspects of the problem to give the reader a better understanding of the FPTDP-EB. Such aspects are the EB's energy consumption, how we modeled the stations, and how we considered solar irradiance and power outages. We note that the technical design of the EB, the stations, or any of their components is not the focus of our research, this section simply explains how we modelled them within our optimization problem.

3.1. Energy consumption

As previously stated, the shorter energy autonomy of EVs than that of ICVs is still one of the former's limitations. The energy consumption of EBs depends on different variables. Two of the most important out of such variables are the speed and weight of the vehicle (Minami and Yamachika, 2004). The weight of the EB has a constant and a variable part. The former is given by the hull and equipment of the boat, which is not selected during this problem. The variable part depends on the number of passengers currently on board and the EB's battery, as the latter is a decision variable of our research. The speed of the EB affects both the consumption and the scheduling of the vehicle. Therefore, the speed of the EB is a decision variable in this research. Such speed refers to that measured relative to the water. For the actual speed of the EB relative to the ground, the river current is either added or subtracted depending on the flow of water. For an equal speed and weight of the boat, the consumption rate during the outward and return trips remains the same. However, the actual energy consumed for trips that go against the current is greater as the travel times are longer.

As mentioned by Villa and Montoya (2018), consumption estimations are required to solve certain transportation problems. For the FPTDP-EB, we require such estimations to be in terms of the EB's weight and speed. There are multiple energy consumption models for boats in the literature. The model chosen for a certain boat depends on whether it has a displacement or planing hull. The former type always displaces the same amount of water to float. The latter generates a lift force at certain speeds, decreasing the amount of displaced water and, by extension, the generated drag (Molland et al., 2017). The EB of our case study has a planing hull. Therefore, we used the model of Savitsky (1964), which is used for planing boats, to estimate the EB's consumption. Although we used this model, as the energy consumption is a parameter of the FPTDP-EB, any other consumption model that depends on the speed and weight of the EB could be used for future implementations of this problem.

Table 1
Strategic optimization problems with EBs.

Considered components	Zhang et al. (2017b)	Lukuyu et al. (2020)	Villa et al. (2020)	Vélez et al. (2020)	Present work
EB's battery sizing		x	x	x	x
Stations location	x	x	x	x	x
PVCSs		x	x	x	x
Sizing of PV components				x	x
Multiple trips of the EB					x
EB's speed decisions					x
EB's scheduling decisions					x
Dealing with stochastic solar irradiance					x
Stochastic number of passengers for the EB					x
Power outages					x

3.2. Charging stations

As mentioned before, we considered two types of stations in this research: SCSs and PVCSs. For SCSs, the only sizing decision to make is selecting their charging power. Such charging powers are defined in terms of the C rates. When charging an electric battery, the C rate indicates the relation between the charging power and the battery's capacity (Battery University, 2017). For a 100 kWh battery, a 1 C rate indicates a charging power of 100 kW, whereas a 0.5 C rate represents a 50 kW power. However, the energy level versus the charging time of electric batteries during a charging process is not constant but follows a nonlinear curve to prevent such batteries from degrading due to overcharging. Such charging processes follow a two-phase behavior referred to as constant current–constant voltage. During the first phase, the charging power is kept almost constant, whereas during the second phase, it is decreased as the battery reaches its maximum capacity (Montoya et al., 2017). All stations are divided into three levels given by their charging powers, with level 1 stations having the lowest powers and level 3 the highest ones (U.S. Department of Energy, 2015). The latter perform their charging operations in direct current (DC). As ENERGETICA 2030 requires relatively short charging times for the EB, we considered only level 3 stations in this research. Therefore, the following explanation focuses solely on level 3 stations. In the case of PVCSs, a portion of the energy they used comes from PV panels. PVCSs require some additional decisions compared with SCSs related to the sizing of their components. Because of this additional sizing, we describe the components of PVCSs and how these stations operate.

The main components of a PVCS are its PV panels, DC–DC converters, and an ESS (optional). PV panels are grouped by arrays, each requiring a DC–DC converter with a maximum power point tracker. This tracker sets the output voltage and current of a PV array to get the maximum power out of it (Cristaldi et al., 2012). DC–DC converters must be appropriately sized for them to endure the maximum power that the PV array may generate. To integrate the PV generation with the charging power of a PVCS, the output voltage of the PV arrays and DC–DC converters must

meet the charging voltage of the station. To do so, we considered that the PV arrays and DC–DC converters are grouped by arrays of series, as in Macellari et al. (2013). Then, when the required voltage is met, any subsequent PV components to be installed must also be grouped in the same arrays of series, which are then connected in parallel to maintain the desired voltage. A PVCS may use an ESS to store any surplus from its PV generation (Bhatti et al., 2016). This energy can then be used when charging an EV for less energy consumption from the grid. When locating a PVCS in the FPTDP-EB, the station's number of PV arrays (and therefore required DC–DC converters), ESS capacity, and charging power must be sized. Fig. 2 shows a diagram of a PVCS with 2 arrays of components connected in parallel, each one having 3 series connected sets of PV panels and DC–DC converters. Numbers in the names of the components simply represent the series and parallel connection that each component belongs to. A public transformer supplies energy in alternate current (AC) from the grid to an internal AC–DC converter that grid-connected charging stations have. The arrays of parallel and series connected PV components and the ESS are then connected in parallel with the internal AC–DC converter to supply energy to the station's charger.

Understanding how energy flows in PVCSs is crucial in solving the optimization problem. The following explanation assumes a PVCS with an ESS, as the scenario without it simply requires that such component is ignored. In our fluvial operation, a PVCS prioritizes using energy mainly from its PV panels, followed by its ESS if needed, and, lastly, buying energy from the grid only if the other sources cannot meet the energy demand. The ESS is charged only by energy surplus from the PV generation and never from the electric grid. If the ESS is fully charged and the EB is not charging, the PV generation is wasted. To protect the ESS from degrading, it is disabled and stops supplying energy if discharged past a given minimum energy level. To enable it back, the ESS needs to be charged past a given nominal energy level. If the ESS is disabled, the EB can still be charged from the PV generation and the energy from the grid.

3.3. Solar irradiance

Solar irradiance is the amount of light energy from the sun that hits a square meter of the Earth each second (NASA, 2008) and is the input for PV generation. The portion of solar irradiance that actually reaches the Earth's surface is stochastic in nature due to weather-related variables such as cloudiness (Ramakrishna and Scaglione, 2016). Fig. 3 compares the solar irradiance profile for a sunny day with that of a cloudy one in Magangué. Therefore, accounting for such stochastic behavior is important to avoid overestimating the PV generation.

Considering that the fluvial transport operation that we design will operate for a significant time horizon, it is important to assess if the solar

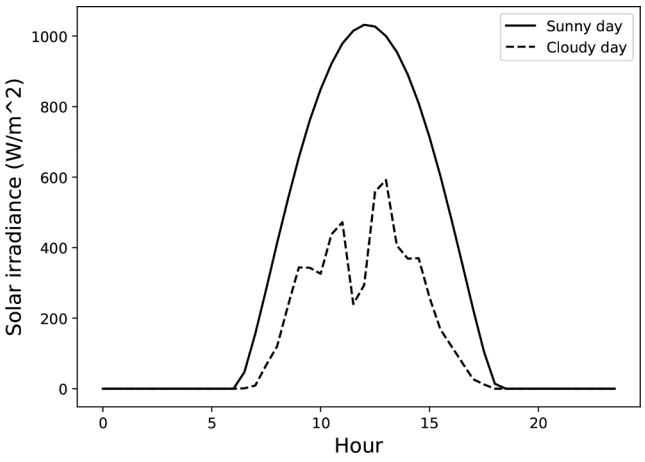

Fig. 3. Solar irradiance profiles during a sunny and a cloudy day in Magangué (data taken from NSRDB (2022)).

irradiance data of the target region presents some tendency or periodicity. In this research, we use half-hourly measured historical data of solar irradiance from the region near Magangué from 1998 to 2017 taken from NSRDB (2022). We first evaluated if the data tended to either increase or decrease over time. To do so, in Fig. 4, we plotted the moving average of the daily average values of solar irradiance over a one-year window. For such daily averages, only the data with greater than 0 irradiance for each day were considered. The vertical dashed lines divide each pair of years. The data do not show either a positive or negative tendency over the analyzed 20-year span. Given this statistical finding, it is plausible to think that future solar irradiance data should not significantly increase or decrease compared with historical values.

Although the target region of the study case does not experience four seasons (as it is located in a tropical zone), it does experience certain weather phenomena such as rainy seasons. Therefore, it was necessary to evaluate if the data presented some periodicity over time. We plotted the daily average solar irradiance values for the whole series to assess if solar irradiance shows some periodicity given by such weather phenomena. In Fig. 5, we take a sample of such values from 2012 to 2017. The black series is the moving average over a window of 14 days, the gray one is the time series as is, and the vertical gray dashed lines are the divisions between each pair of years. Solar irradiance seems to show a certain yearly periodicity. For example, the first months in each year tend to have high irradiance (dotted circles), and two seasons of low average irradiance can be seen yearly, starting around late April and early October (continuous circles).

Each candidate solution for the FPTDP-EB, which has at least one

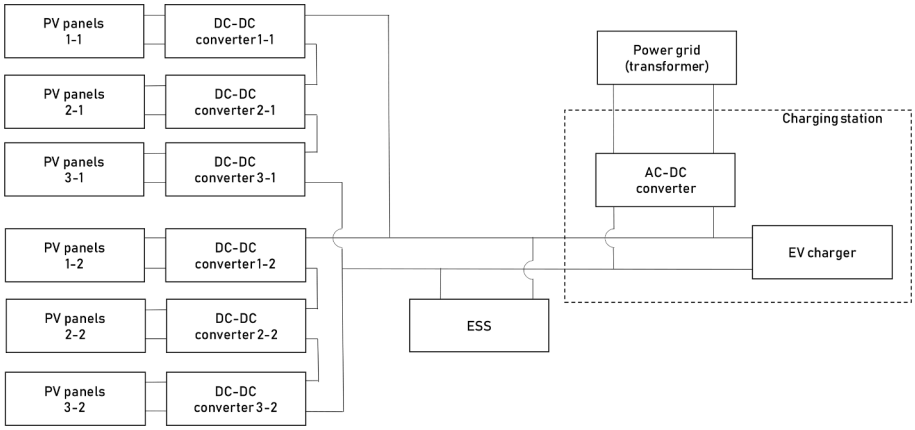

Fig. 2. Diagram of the connections of the components of a PVCS.

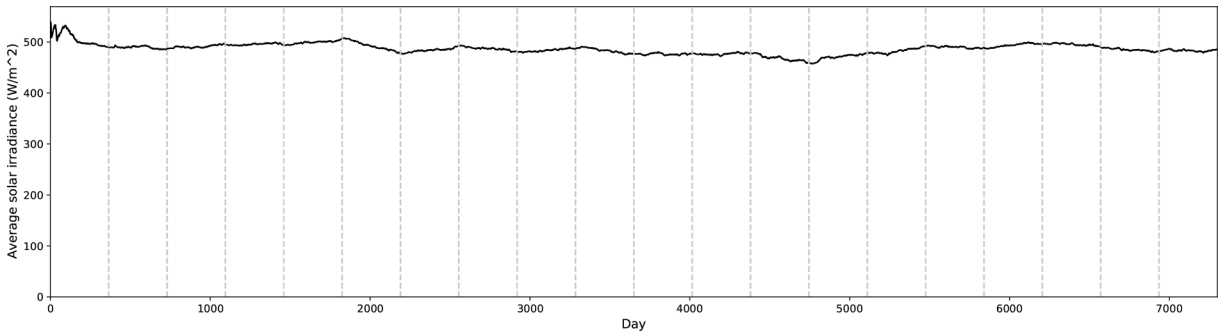

Fig. 4. Tendency of Magangué's daily average solar irradiance (data taken from NSRDB (2022)).

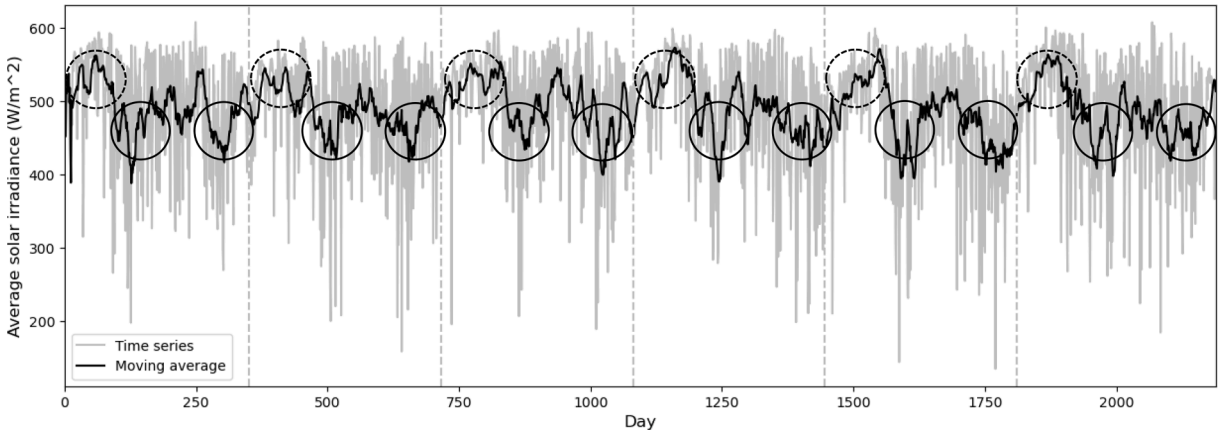

Fig. 5. Periodicity of daily average solar irradiance in Magangué (data taken from NSRDB (2022)).

PVCS, must be evaluated considering the solar irradiance behavior during a given time horizon. Such evaluation must take into account the periodicity of the irradiance. A simple yet effective way of doing so is to use historical data during the evaluation. This is valid as the data do not tend to either increase or decrease with the passage of years. Using this historical data allows us to guarantee that we do not evaluate a day with a behavior present during the middle of a year followed by one corresponding to the end of a year (which have significantly different behaviors). This strategy guarantees that if a certain weather condition (e.g., a rainy season) occurs, all consecutive days reflect the same behavior. Solar irradiance is multiplied by a PVCS's total area of PV panels and the panels' efficiency to estimate the PV generation during each moment of a day for the FPTDP-EB.

3.4. Power outages

As previously mentioned, rural areas tend to have less reliable electric grids than urban areas, increasing the chances of a power outage occurring. We considered such outages in our model. We did so using two stochastic variables: the time between power outages and their duration (Agrawal, 2018). We used an indicator called the system average interruption frequency index (SAIFI), which indicates the average number of power outages per consumer of a power supplier during a given period, to estimate the associated probability distributions of the time between outages (Superservicios, 2017). For the probability distributions of the outages' duration, we yet again used the SAIFI and another indicator called the system average interruption duration index (SAIDI), which is the total amount of time that the average consumer of a certain power supplier experienced power outages during a time period (Superservicios, 2017). The average duration of the power outages was then the SAIDI divided by the SAIFI.

4. Problem description

As mentioned in Section 1, the FPTDP-EB makes both infrastructure- and scheduling-related decisions. We first define the sets and parameters related to the infrastructure decisions. Let B represent the set of battery capacities that may be selected for the EB. Let d_b^{BAT} be the cost of a battery with capacity $b \in B$. Let $N = \{0, \ldots, n\}$ be the set of candidate nodes where stations may be installed. Let nodes 0 and n be ports where passengers may board or disembark the EB, regardless of whether a station is installed at either of them. The outward trip starts at 0 and ends at n and vice versa for the return one. As previously mentioned, we considered that the stations to be installed in this problem could be either SCSs or PVCSs. Regardless of its type, each station may only have one charging power. The charging powers to consider for the stations are related to the EB's battery capacity to allow certain charging times to be achieved. This is so that an EB with a large battery capacity is not charged with relatively low charging power. Let then Q_b be the set of charging powers for the stations when the EB has a battery capacity $b \in B$. Let d_q^{CP} be the cost of a station given by its charging power $q \in Q_b$ when the EB has a battery capacity $b \in B$. Additionally, let d^M be the estimated yearly maintenance cost for a station. We consider this cost to be the same for each station. For PVCSs, the number of PV arrays and the capacity of the ESS must also be determined. Therefore, the costs of such components must be added to those given by their charging power. Regarding the number of PV arrays, let P_i be the set of configurations of PV arrays that may be installed for a PVCS at node $i \in N$, given the logistical limitations of such node. Let d_p^{PV} be the cost of the configuration of PV arrays $p \in P_i$ that may be installed for a PVCS at node $i \in N$. Such cost also accounts for the required DC–DC converters due to the configuration of the PV arrays. As mentioned before, PVCSs may optionally have an ESS to store their PV generation. The ESS's capacities

to be considered are also related to the EB's current battery capacity to avoid ESS capacities that are either relatively low or even greater than those of the EB's battery. Let then E_b be the set of ESS capacities that may be selected for a PVCS when the EB has a battery capacity $b \in B$. Let d_e^{ESS} be the cost of an ESS $e \in E_b$ when the EB has a battery capacity $b \in B$.

We now define the sets and parameters related to the scheduling decisions. Let S be the set of speeds at which the EB may travel. As mentioned before, the energy consumption of the EB depends on the speed and weight of the EB. Let then g be the number of passengers aboard the EB during a given trip and $\bar{g}$ the maximum passenger capacity of the EB. Also, let N' be a subset of N containing the nodes where a station is installed. Let then $\overrightarrow{\theta_{bisg}}$ be the energy consumption of the EB when traversing between nodes i and $suc(i)$ $\forall i, suc(i) \in N' \cup \{0, n\}$, with $suc(i)$ being the successor of i, during the outward trip while having a battery with capacity $b \in B$ and speed $s \in S$ and transporting g passengers. Likewise, let $\overleftarrow{\theta_{bisg}}$ be the energy consumption when traversing between nodes $suc(i)$ and i $\forall i, suc(i) \in N' \cup \{0, n\}$ during the return trip. Nodes 0 and n must be accounted for in both of the consumption parameters regardless of whether they have an installed station to track the consumption during the whole round trip. As mentioned in Section 3.3, even though solar irradiance is stochastic in nature, as the FPTDP-EB spans over multiple years where the periodicity of the data must be accounted for and given the data's lack of tendency to either increase or decrease, we used historical data of the target region's solar irradiance for the simulation. As mentioned in Section 1, this problem aims to use an EB to perform a fluvial operation now performed using ICBs. Such ICBs do not follow fixed departure schedules but rather depart once a given number of passengers have boarded. However, at the time of this writing, this aspect causes passengers to have to wait an undefined amount of time for an ICB to depart, which sometimes even means waiting between days. Therefore, to provide a better quality of service for the passengers, the FPTDP-EB proposes some fixed departure times for the EB. Thus, let H be the set possible daily departure times from node 0. Also, let Δ be the amount of time that the port in node 0 is open during each day. To estimate the waiting time of passengers as a quality service measure, we considered the arrival time of passengers to the ports as a random variable. We also considered the possibility of having power outages, which are modeled using two random variables: the time between outages and their duration.

The objective function of the FPTDP-EB is to minimize the total operational cost. This cost is the sum of the investment costs for the EB's battery and the stations, the maintenance cost of the latter and the costs of the energy to be purchased from the grid during a given number of years of the EB's operation. For a solution to be feasible, the probability of having a feasible day of the EB's operation must be greater than or equal to α, as in chance-constrained programming (Oyola et al., 2018). For a day to be feasible, the energy autonomy of the EB must be met at all times and certain service-quality-related constraints must not be violated. These service quality constraints consist of transporting a minimum percentage λ of passengers during the day, keeping the average waiting times below a certain maximum value τ and performing a minimum number ρ of round trips daily. The latter of these constraints is targeted towards providing future decision makers of the operation with an additional tool that can help them tailor a solution closer to their needs. For example, having the minimum number of round trips could help decision makers explore solutions that provide more departure time alternatives for passengers (i.e., more trips), which could be a potential differentiator against competitors.

To provide a better understanding of the FPTDP-EB, Fig. 6 shows an illustrative example of a solution to the problem. In the example we have $N = \{0, 1, 2, 3\}$, with nodes 0 and 3 being ports where passengers may board or disembark the EB. A PVCS with charging power of 1 C (in C rate), a configuration of 15 PV arrays and an ESS of capacity 75 kWh was installed in node 0, while a SCS with charging power 0.5 C was installed in node 2. A battery with capacity of 150 kWh was selected for the EB. For the traveling speeds, 50 km/h and 45 km/h were the selected speeds for the outward and return trips. Finally, two round trips where scheduled for the EB with departure hours at 10:00 and 13:30.

5. A simulation-based branch-and-bound algorithm

Considering the strategic side of the FPTDP-EB, we decided to use an exact optimization method to make the decisions of the problem. We propose a two-stage simulation-based branch-and-bound algorithm as our solution approach. The first stage determines the infrastructure and scheduling decisions and calculates the investment costs plus the maintenance cost of the charging stations (which is a fraction of the objective function) using a branch-and-bound algorithm. Branch-and-bound algorithms are a family of exact optimization algorithms that implicitly explore a problem's solution space using a tree structure. Implicit exploration means that not every possible solution is evaluated, as using a set of rules called pruning rules, some suboptimal or infeasible solutions are detected before being evaluated (Morrison et al., 2016). During the second stage of our solution method, each candidate solution that the branch-and-bound provides is evaluated using a Monte Carlo simulation. This simulation assesses the feasibility of the solution and estimates the cost of energy to purchase from the grid (the other fraction of the objective function) making the charging decisions of the operation. These charging decisions must be manually performed by the EB's driver. Because of that, we opted for some smart charging decisions which can be easily implemented by the driver, even though they may not be optimal. Additionally, evaluating the feasibility of the operation on the optimal charging decisions may be risky if such decisions are hard to implement. Therefore, given that the branch-and-bound algorithm implicitly explores every combination of the decision variables, we provide the best solution for the FPTDP-EB considering that the charging decisions are not optimal. These charging decisions are explained in Section 5.2.

Branch-and-bound algorithms have been used to solve different

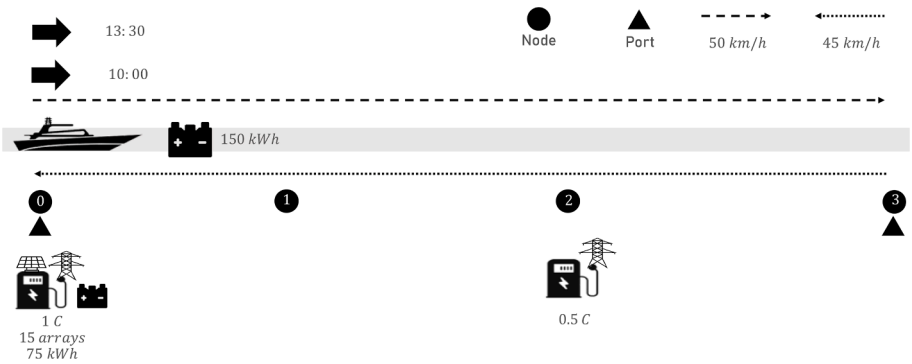

Fig. 6. Example of the FPTDP-EB.

optimization problems. In transportation topics, Hu et al. (2016) used a branch-and-bound algorithm to minimize the cost and time of freight transportation for a transportation service procurement problem. Recently, Soto et al. (2020) used a parallel branch-and-bound algorithm to reduce the completion time, maximum workload, and summed workload of a set of machines for a multiobjective flexible job-shop scheduling problem. Using a simulation-based branch-and-bound algorithm, Espinouse et al. (2000) solved a job input sequencing and device dispatching problem in a flexible manufacturing system. Their approach was also two-staged, with the first stage solving the job input sequencing via a branch-and-bound-algorithm. Their second stage uses a discrete event simulation model to determine the vehicle scheduling for the dispatching and to evaluate the performance of the system and the makespan.

The rest of Section 5 explains our solution method. Section 5.1 describes the first stage of our solution method, the branch-and-bound algorithm. Section 5.2 explains the second stage of the solution method, the Monte Carlo simulation that evaluates each candidate solution.

5.1. First stage: branch-and-bound algorithm

This section is divided into two parts. The first part presents the general structure of the branch-and-bound algorithm while the second one describes the pruning rules. Some of these rules compare a dual bound of the problem to the primal bound while others evaluate the feasibility of a partial solution.

5.1.1. General structure

We selected the depth-first search variant for our branch-and-bound algorithm. This algorithm calls three types of functions. The first are groups of pruning rules, each of which returns a boolean value equal to true if the current branch is worthy of further exploration and false if it must be pruned. These groups are given the type of decision that each rule evaluates, which will be explained in Section 5.1.2. The second type of functions is the investment cost calculation. The investment cost calculation returns the cost a of the EB's battery and the charging infrastructure (plus its maintenance cost). The third type of functions is the second stage of the solution method, the Monte Carlo simulation. This function evaluates each candidate solution and returns a boolean value u indicating if the solution is feasible and the cost of the energy to be purchased from the grid, r.

Algorithm 1 describes the general structure of our branch-and-bound algorithm. The algorithm starts by initializing the variable *Best* and the list S_{best} (lines 2 and 3). The latter stores the best solution found so far. Then, the algorithm iterates over a set of battery capacities (line 4). For each capacity $b \in B$, the algorithm evaluates whether a search should be continued in a particular branch using the function `PruningRulesBattery`(b,S,P,E_b,Q_b,N) (line 5). The algorithm then iterates over all possible combinations of selected nodes in which a station (N') is to be installed out of set N (line 6). The function `PruningRuleNodes`(b,N') evaluates whether a current branch should be further explored given by a current set N'. The algorithm continues by iterating over the set of stations' technologies (line 8). A station's technology consists of its charging power $q \in Q_b$, number of panel arrays $p \in P_i$, and ESS capacity $e \in E_b$. The last two only apply to PVCS. $\Pi_{N'}$ represents the set of all the possible technologies that can be installed at nodes N'. An element $\pi_{N'} \in \Pi_{N'}$ is a list of size $|N'|$ where each element stores the components of the station (q,p,e). Assuming a problem with 3 nodes and $N' = \{2,3\}$, an example of $\pi_{N'}$ is $\{(10kW, 20m^2, 5kWh), (20kW, -, -)\}$, where the station located at node 3 is an SCS. After selecting the technologies for the selected nodes N', the algorithm calls the function `PruningRulesCSs`$(b,\pi_{N'})$ to evaluate whether the search continues in such branch (line 9). The algorithm then iterates over the set of speeds S (line 10). The algorithm checks the pruning rules of the speeds decision with the function `PruningRulesSpeeds`$(b,\pi_{N'},s_o,s_r)$ (line 11), with s_o and s_r being the selected speeds during the outward and return trips, respectively. The algorithm then moves to the departure times decision loop (line 12). For this decision, let H' be a subset of H having the currently selected departure times.

For each possible $H' \subset H$, the algorithm calls the function `PruningRulesHours`$(b,\pi_{N'},s_o,s_r,H')$ to check whether its execution should be continued. Then, the function `InvestmentCostCalculation`$(b,\pi_{N'})$ calculates the cost a of the EB's battery plus the charging infrastructure (line14). After that, the function `Simulation`$(b,\pi_{N'},s_o,s_r,H')$ evaluates the current candidate solution (line 15). If the solution is feasible and its cost is less than *Best*, both *Best* and S_{best} are updated (lines 16 to 18). Finally, the algorithm returns *Best* and S_{best} (line 30).

Algorithm 1: Branch-and-bound algorithm general structure

```
1: function Branch_and_bound N,B,P,E_b,Q_b,S,H
2:   S_best ⟵ ⟨⟩
3:   Best ⟵ ∞
4:   for each b ∈ B do
5:     if PruningRulesBattery(b,S,P,E_b,Q_b,N) =true then
6:       for each N' ⊂ N do
7:         if PruningRuleNodes(b,N') =true then
8:           foreach π_N' ∈ Π_N' do
9:             if PruningRuleCSs(b,π_N') =true then
10:              for each s_o and s_r ∈ S do
11:                if PruningRulesSpeeds(b,π_N',N',s_o,s_r) =true then
12:                  for each H' ⊂ H do
13:                    if PruningRulesHours(b,π_N',N',s_o,s_r,H') =true then
14:                      a ⟵ InvestmentCostCalculation(b,π_N')
15:                      ⟨u,r⟩ ⟵ Simulation(b,π_N',s_o,s_r,H')
16:                      if u = true and a+r < Best then
17:                        Best ⟵ a + r
18:                        S_best ⟵ ⟨b,N',π_N',s_o,s_r,H'⟩
19:                      end if
20:                    end if
21:                  end for
22:                end if
23:              end for
24:            end if
25:          end for
26:        end if
27:      end for
28:    end if
29:  end for
30:  return S_best, Best
31: end function
```

Table 2 summarizes the decisions of the FPTDP-EB with the specific notation that we used for them within Algorithm 1. To make the table clearer, we added a third column to it with the values that we used in the illustrative example at the end of Section 4.

5.1.2. Pruning rules

Each pruning rule returns a boolean value equal to true if the branch-and-bound algorithm's search in a current branch is worthy of

Table 2
Decisions of the FPTDP-EB.

Decision	Notation	Value in the example
Selected battery capacity for the EB	$b \in B$	150 kWh
Set of nodes where a station is installed	$N' \in N$	[0, 2]
List of the selected components for each station	$\pi_{N'} \in \Pi_{N'}$	[[1 C, 15 arrays, 75 kWh], [0.5 C, 0 arrays, 0 kWh]]
Selected speed to traverse the outward trip	$s_o \in S$	50 km/h
Selected speed to traverse the return trip	$s_r \in S$	45 km/h
Set of selected daily departure departure hours for the EB	$H' \in H$	[10:00, 13:30]

continuing and false if such branch must be pruned. As mentioned before, the pruning rules were grouped according to the type of decisions they help take. Each function returns a boolean value true only if every single one of its pruning rules returns true on itself. This section defines each of the pruning rules in their respective groups.

Battery capacity pruning rules

The following two rules account for the battery capacity that is currently being evaluated, b^*. They are both grouped in the function `PruningRulesBattery`(b^*, S, P, E_b, Q_b, N) in Algorithm 1.

- **Pruning rule** $b1$**:** This rule checks if the battery capacity b^* would allow at least one feasible solution to the problem to exist when installing stations at every node in N with the best possible configuration of technologies $\overline{\pi_N}$. This configuration consists of installing PVCSs with the highest number of PV array $\overline{p} \in P$, the highest ESS capacity $\overline{e} \in E_{b^*}$, and the highest charging power $\overline{q} \in Q_{b^*}$. This best configuration requires all stations to be PVCSs due to the possibility of power outages. The rule runs the function $\langle u, r\rangle \longleftarrow$ `Simulation` $(b^*, \overline{\pi_N}, s_o, s_r, H')$ for every possible combination of speeds s_o and $s_r \in S$ and list of departure times $H' \subset H$. If u is true for a given combination of s_o, s_r, and H', there exists a feasible solution to the FPTDP-EB having b^*. Therefore, $b1$ returns true. Additionally, the rule instantly stops its execution. If every possible combination of s_o, s_r, and H' is evaluated without u ever being true, $b1$ returns false.
- **Pruning rule** $b2$**:** This rule returns true if the cost of a battery with capacity b^* is less than the cost of the current best solution (i.e., $d_{b^*}^{BAT} < Best$). Otherwise, it returns false. Such cost of the battery with capacity b^* is a dual bound for the problem.

Node pruning rule. This group has only one pruning rule and is represented in the function `PruningRuleNodes`(b^*, N).

- **Pruning rule** $n1$**:** This rule returns true if the EB would be able to traverse the distance between each pair of installed stations in N' at the lowest possible speed $\overline{s}$. This speed is selected to consider the scenario with the lowest consumption. We assume the number of passengers to be $\overline{g}$ as the EB must withstand such occupancy. Given that batteries should not be fully discharged because of battery health reasons (Hossain et al., 2019), let z be the usable amount of energy from a battery with capacity b^*. Additionally, let ζ be the second-to-last element in set $N' \cup \{0, n\}$. The rule returns true only if all of the following hold true.
  - i $\overrightarrow{\theta_{b^*i\overline{sg}}} \leqslant z, \forall i, suc(i) \in N' \cup \{0, n\}$
  - ii $\overleftarrow{\theta_{b^*i\overline{sg}}} \leqslant z, \forall i, suc(i) \in N' \cup \{0, n\}$
  - iii $\overrightarrow{\theta_{b^*,\zeta,\overline{sg}}} + \overleftarrow{\theta_{b^*,\zeta,\overline{sg}}} \leqslant z$.

  Expression (i) checks if the amount of usable energy of the battery would allow the EB to depart from port 0, traverse between each pair of stations, fully charging at each of them, and arrive at port n during the outward trip. Likewise, expression (ii) does the analogous validation for the return trip. Expression (iii) checks if the amount of usable energy of the battery would allow the EB to traverse back and forth from the station closest to port n. Condition (iii) must only be evaluated if $n \notin N'$. It must otherwise be ignored. This is because the EB would only be forced to traverse such distance without recharging if there is not a station in node n.

Stations pruning rule. This group also has only one pruning rule. It evaluates the current configuration of the stations' technologies $\pi_{N'}^*$ and is represented in the function `PruningRuleCSs`$(b^*, \pi_{N'}^*)$.

- **Pruning rule** $c1$**:** This rule returns true if the cost of a battery with capacity b^* plus the cost of stations with technologies $\pi_{N'}^*$ is less than the cost of the current best solution. Otherwise, it returns false. This cost of the battery plus the charging infrastructure is another dual bound for the problem.

Speed pruning rules. The following two rules account for the speeds currently being evaluated for the outward and return trips s_o^* and s_r^*, respectively. They are both grouped in the function `PruningRulesSpeeds`$(b^*, \pi_{N'}^*, N', s_o^*, s_r^*)$.

- **Pruning rule** $s1$**:** This rule is analogous to $n1$. The rule evaluates the same expressions (i)–(iii) defined for $n1$ simply considering speeds s_o^* and s_r^* rather than $\overline{s}$ for both trips.
- **Pruning rule** $s2$**:** This rule checks that at least the minimum number of daily round trips ρ may be performed timewise. Let ϕ_j be the sum of the total travel time and the minimum time to recharge the energy needed to perform j round trips $\forall j \in Z^+$. Such energy is the difference between the total energy consumption to perform j round trips and z (which is the maximum amount of energy the EB may have before starting its daily operation). We assume the best-case scenario for the charging operations, which is charging with the highest power $\overline{q}$ available in $\pi_{N'}^*$, to consider the minimum charging time. We also assume only one passenger aboard the EB to evaluate the scenario with the lowest possible energy consumption. We note that $\phi_j > j\phi_1 \quad \forall j > 1$ as the first round trip in a day starts fully charged from the previous day, whereas any subsequent round trip in a day would require charging in between trips. The rule returns true if $\phi_\rho \leqslant \Delta$.

Departure time pruning rules. The following two rules account for the list of departure times H' currently being evaluated. They are grouped in the function `PruningRulesHours`$(b^*, \pi_{N'}^*, N', s_o^*, s_r^*, H')$.

- **Pruning rule** $h1$**:** This rule checks the minimum time between the currently selected departure times. Let δ_i be the difference between departure times i and $i+1 \forall i \in \{1, \ldots, |H'|-1\}$. The rule returns true only if $\delta_i \geqslant \phi_1 \forall i \in \{1, \ldots, |H'|-1\}$.
- **Pruning rule** $h2$**:** This rule estimates the maximum number of round trips that could possibly be performed in a given day. The rule searches for the greatest integer k so that $\phi_k \leqslant \Delta$. The rule then returns true if $|H'| \leqslant k$.

5.2. Second stage: Monte Carlo simulation

As mentioned before, during the second stage of our solution method, each candidate solution provided by the branch-and-bound algorithm is evaluated through a Monte Carlo simulation. It simulates the operation of the EB during a given number of years, assessing the feasibility of the solution and estimating the cost of the energy that would be purchased from the grid. In this section, we briefly describe the main components that we considered for the simulation. As previously mentioned, the simulation considers certain stochastic variables. Because of that, multiple replications are executed for each solution. For a solution to be feasible, at least β percent of its replications must be so. This approach was based on the Simulation Route Evaluator by Gómez et al. (2016). For a replication to be feasible, the probability of having a feasible day must be greater than or equal to α. This probability is calculated by dividing the number of feasible days by the total number of simulated days. As mentioned before, for a day to be feasible, all of the scheduled round trips must be finished, the energy autonomy of the EB must be met at all times, at least λ percent of candidate passengers must be transported, and their average waiting time must not exceed τ.

The simulation performs the charging operations that the EB requires. They affect both the feasibility of each day and the energy to be

purchased from the grid. We divide the charging operations into three groups: interday, interroute, and en-route charging operations. The interday charging operations have the EB charging its battery to its maximum capacity. The interroute operations also aim at fully charging the battery but are time-constrained between the arrival hour of the EB during its previous round trip and the scheduled departure time of the following one. These types of charging operations can only be performed if there is a station at node 0. For the en-route charging operations, the energy that the EB would require to travel to the following station is calculated each time it arrives at a given station. The EB charges only if such calculated energy is greater than what is currently available in its battery. If a charging operation is required, the energy to be charged is the minimum amount between the missing energy to arrive at the next station and the amount that may be charged given by the maximum charging time. Such maximum charging time is estimated as the difference between either the time when the following round trip must start or when port 0 closes and the travel time to complete the current round trip. The energy calculation is performed with the current number of passengers at any given time. Therefore, if there is no station at port n and the number of passengers changes in that node, the calculation may not coincide with the actually experienced consumption. As mentioned before, we note that these may not be the optimal charging decisions, but rather some smart ones which may be easily implemented by the EB's driver.

In case there is at least one PVCS, here we consider solar irradiance. As mentioned in Section 3.3, we use the time series of the historical solar irradiance data from the target region, as would be done in a historical simulation. As mentioned in Section 3.2, a PVCS prioritizes using the energy generated from its PV arrays and the one stored in its ESS, in case it has one, buying energy from the grid only if the other two sources are insufficient. The total cost of energy to be purchased from the grid during a feasible solution is then the average of the total costs of each replication. For this simulation, we also consider a random variable for the time between the arrivals of candidate passengers at each port. Such passengers may arrive at a port between its opening hour and an arbitrary hour before the port's closing hour so that people who arrive when a port is about to close are not considered candidates. We considered that candidate passengers remain in the ports during such hours until they may board the EB; they do not leave until the day finishes or take another way of transportation. For each trip, the number of passengers g is decided given the number of candidate passengers in a port at the time of departure, the current energy level of the EB and $\overline{g}$. If the EB is at port n and can transport at least one passenger, the vehicle departs without charging. Otherwise, the EB charges and departs with one passenger. With the number of passengers who boarded and their waiting time, we evaluate the feasibility of a solution due to the service quality constraints. As mentioned before, we also consider another stochastic phenomenon related to the power outages that may occur as the EB will be implemented in a rural area. This time, however, the phenomenon is modeled using two stochastic variables: the time between outages and their duration. These outages pose a higher risk with SCSs as the charging processes stop until the power is restored. On the other hand, PVCSs may continue charging using energy from their PV arrays or ESS during these outages.

6. Computational-experiments

For the case study, we built a base scenario for the problem based on data from other research and field trips from ENERGETICA 2030. In this section, we present such scenario, evaluate its solution, and perform some sensitivity analyses based on it. The latter analyses consist of increasing the minimum number of days that must be feasible per replication, increasing the energy density of the EB's battery, decreasing the average time between outages and increasing their average duration, and, finally, considering a scenario with low solar irradiance. For the execution, we set the number of replications of the simulation to 500 and β to 90%. The algorithm was implemented on Java (java/jdk-1.8.0_112). We published the code in the following public GitHub repository: https://github.com/camilovelez/FTDPEB. Experiments were run on a computing cluster with an Intel Xeon E5-2683 v4 processor (with 32 cores at 2.1 GHz) and 64 GB of RAM running on Linux Rocks 6.2–64 bits - Centos 6.6.

6.1. Scenario description

The fluvial operation is a round trip of about 110 km between Magangué and Pinillos. Apart from such municipalities, a settlement between the two, known as Tanqueo, where ICBs refuel, was selected as a candidate node for installing a station. These three locations form the set N, with Magangué being node 0 and Pinillos node n. The sets and parameters for the base scenario of the case study can be seen in Table 3. The rest of this paragraph clarifies certain sets or parameters we deemed necessary to explain. Most of the parameters were taken from a field research performed by ENERGETICA 2030. As mentioned before, sets Q_b (the set of charging powers) and E_b (the set of ESS's capacities) depend on the current battery capacity of the EB, b. This is done to evaluate some adequate C rates for the EB's battery rather than fixed charging powers and to avoid relatively low or unnecessarily high ESS capacities. We used the same battery technology for both the EB's battery and the ESSs. Therefore, their technical parameters are the same[2]. In Table 3, we display the cost of either a battery of the EB or an ESS in terms of the cost per kWh. Therefore, to get the actual costs d_b^{BAT} and d_e^{ESS}, multiplying such costs per kWh by either the battery's of the ESSs' capacities is necessary. For the stations, we estimated their costs given by their charging power with a linear regression using data for the costs of components of 50-, 150-, and 350-kW stations taken from Nicholas (2019). As previously mentioned, the cost d_p^{PV} of a PVCS accounts for both the PV arrays and the DC–DC converters. In Table 3, the costs of such components are presented separately, with the cost of the PV arrays being that of a single PV panel times the number of installed ones. Also, for PVCSs, the number of PV panels per array of series to guarantee the desired charging voltage was estimated using the range of voltages accepted by the EB's battery and the parameters of the converter (Solartex, 2020a). We considered that the maintenance cost of the stations brought to present value did not change. We simulated 8 years of the fluvial operation, which is the battery's expected lifespan according to its warranty. We considered the time between passengers' arrivals to follow an exponential probability density function (PDF). According to the field research, people were more likely to arrive at the ports during the morning and the afternoon rather than at noon. Therefore, we defined J as the set of such time periods of each day. Let μ_{ij} be the average time between passenger's arrivals at port $i \in \{0, n\}$ during the time period $j \in J$. The field research did not find a significant difference between passenger arrivals at ports 0 and n. Thus, we set $\mu_{0j} = \mu_{nj} \forall j \in J$. The cost of energy from the grid was estimated using another linear regression, using the monthly energy bills from 2014 to 2020 of Magangué's power supplier taken from Afinia (2022). We estimated different energy costs for each of the following 8 years. Such costs were then brought to present value to be summed with the investment costs. Additionally, we considered a tax for the CO_2 emissions of the energy from the grid. Such tax in Colombia is charged only to the use of hydrocarbons and not to energy generation. We simply included it to further incentivize the use of PV energy. We considered both the time between events and their duration to have exponential PDFs for the power outages. Their parameters were estimated using the SAIDI and SAIFI of Magangué's power supplier from 2016 to 2018, taken from Superservicios (2017) and Superservicios (2019).

[2] The name of the supplier was treated as undisclosed commercial information

Table 3
Parameters for the base scenario.

	Parameter	Values	Units	Data source
Sets	Battery capacities (B)	104, 130, 156, 208	kWh	Field research
	Nodes (N)	0, 1, 2		Field research
	Charging powers to be evaluated (Q_b)	0.5, 1	C rate	Field research
	Number for the PV arrays (P)	14, 21	Arrays	Field research
	ESS capacities to be evaluated (E_b)	0, 50, 100	% of b	Field research
	Speeds (S)	20, 30, 40, 50	km/h	Field research
	Departure times (H)	6:00, 8:00, 10:00, 12:00, 14:00, 16:00	Time	Field research
	Time periods of the day (J)	6:00–9:20, 9:20–12:40, 12:40–16:00	Time	Field research
Electronic components	Battery energy density	0.18	kWh/kg	Supplier's quotation
	Cost per kWh of the batteries	254.81	USD/kWh	Supplier's quotation
	Min energy level percentage for batteries	5	%	Field research
	ESSs' nominal energy level percentage	20	%	Field research
	Cost of a station given by its charging power (d_q^{CP})	Linear regression	USD	(Nicholas, 2019)
	Cost of a PV panel	163	USD	(Solartex, 2020b)
	Area of each PV panel	2.24	m^2	(Solartex, 2020b)
	PV panel efficiency	20.71	%	(Solartex, 2020b)
	Number of PV panels per array	6	Panels	Field research
	Cost of a DC–DC converter	266.5	USD	(Solartex, 2020a)
	Number of PV arrays to connect in series	7	Arrays	Estimated
	Yearly maintenance cost for a station (d^M)	800	USD	(AFDC, 2018)
Scheduling parameters	River speed (flows from Pinillos to Magangué)	3	km/h	Field research
	Weight of the EB without its battery	1790	kg	Field research
	Weight per passenger	92	kg	Field research
	Port 0 opening hour	6:00	Time	Field research
	Port 0 closing hour	18:00	Time	Field research
	Last hour for candidate passengers to arrive	16:00	Time	Field research
	PDF for the time between passengers' arrivals	$\text{Exp}(\mu_{ij})$		Field research
	Mean time between passengers' arrivals (μ_{0j} and μ_{nj})	0.27, 0.54, 0.27	h	Field research
	Average number of daily passengers per port	16	Passengers	Field research
	EB's max number of passengers ($\overline{g}$)	8	Passengers	Field research
	Min required number of daily round trips (ρ)	1	Trips	Field research
	Number of simulated years	8	Years	Battery's warranty
	Min percentage of feasible days per replication (α)	90	%	Field research
	Min percentage of passengers to transport daily (λ)	33	%	Field research
	Max average waiting time for passengers (τ)	5	h	Field research
Energy params.	Cost of energy bought from the grid	Linear regression	USD/kWh	(Afinia, 2022)
	Inflation rate	3	%	(MinHacienda, 2017)
	CO_2 emission per kWh of generated energy	0.381	$kgCO_2$/kWh	(UPME, 2020)
	Tax per emitted kg of CO_2	0.00369	USD/$kgCO_2$	(Portafolio, 2018)
	Solar irradiance data	Data from 2010 to 2017	kW/m^2	(NSRDB, 2022)
	PDF for the time between power outages	$\text{Exp}(83.4)$		Estimated
	PDF for duration of power outages	$\text{Exp}(1.01)$		Estimated

6.2. Performance of the simulated-base branch-and-bound algorithm

Before analyzing the solution of the base scenario, we want to evaluate the computational performance of the simulated-base branch-and-bound algorithm and the effect of having the pruning rules on such scenario. Thus, Table 4 shows the speedup of the solution when activating and deactivating certain pruning rules. The speedup is calculated as the CPU time of the execution without any pruning rules divided by the CPU time of each particular execution. Crosses in Table 4 show which rules were active during a certain execution. When no pruning rules were active, the CPU time was 19.39 h, whereas the execution with all of the pruning rules active was 2.9 h, which gives a speedup of 6.69. It can also be seen that each pruning rule helped decrease the CPU time. Given the strategic nature of the FPTDP-EB, a 2.9 h execution time is reasonable in solving the problem.

Table 4
Pruning rules speedup.

Departure Times		Speeds		Stations		EB's Battery			
$h1$	$h2$	$s1$	$s2$	$c1$	$n1$	$b1$	$b2$	CPU time (h)	Speedup
								19.39	
x								5.17	3.75
x	x							4.39	4.42
x	x	x						4.11	4.72
x	x	x	x					3.69	5.25
x	x	x	x	x				3.46	5.6
x	x	x	x	x	x			3.43	5.65
x	x	x	x	x	x	x		2.93	6.62
x	x	x	x	x	x	x	x	2.9	6.69

6.3. Results

The solution of the base scenario can be seen in Tables 5 and 6. Table 5 presents the general attributes of the solution of the base scenario. An intermediate value of b was selected, which shows that some savings are made by properly sizing the battery. The solution installed a station at every candidate node due to the capacities for the EB's battery and the energy density of such component that were evaluated in our case study. However, in Section 6.4 we show that fewer stations are installed when considering a greater battery energy density, greatly decreasing the overall cost of the solution. All of the installed stations in the solution were PVCSs. Given that the EB's daily operation (which is

Table 5
General attributes of the solution of the base scenario.

Attribute of the solution	Value
Battery capacity of the EB (b)	130 kWh
Stations installed	3
Speed during the outward trip (s_o)	50 km/h
Speed during the return trip (s_r)	50 km/h
Departure hours (h)	10:00 and 14:00
Energy to purchase from the grid	92,209.3 kWh
Total cost	269,123.5 USD
Cost of the EB's battery (d_b^{BAT})	33,125.35 USD
Cost of the stations (including their maintenance)	223,483.15 USD
Cost of the energy to purchase from the grid	12,515.01 USD

Table 6
PCVS related attributes of the solution of the base scenario.

Attribute of the solution	Magangué	Tanqueo	Pinillos
Number of PV arrays (arrays)	14	14	14
ESS capacity (% of b)	100	50	50
Charging power (C rate)	1 C	1 C	1 C

detailed in the following paragraph when explaining Fig. 7) is rather tight timewise, the maximum speed was chosen for both s_o and s_r. Such operation required two daily round trips, with departure hours at 10:00 and 14:00, to meet service quality constraints. Looking at the total cost, 83.04% of it was spent on the PVCSs, 12.31% on the EB's battery, and 4.65% on the energy to purchase from the grid. Even though there was a large investment in PV components, the savings in the amount of energy to purchase from the grid make up for it. Table 6 shows the attributes of the solution of the base scenario that are related to the PVCSs. The PVCS in Magangué had the greatest ESS capacity out of the three. This is due to the amount of energy charged per charging operation, as the average charging operation in Magangué charged 98.89 kWh. In comparison, the averages in Pinillos and Tanqueo were respectively 75.77 and 51.33 kWh. Additionally, the maximum charging power was installed at each PVCS, which is yet again due to the tight schedule of the EB.

Fig. 7 shows three consecutive days of such operation using a Gantt-chart-like structure to evaluate and understand the daily operation of the EB. Tasks T1 (black bars) represent the charging processes, whereas tasks T2 (gray bars) represent the EB traveling between nodes. The amount of energy charged during each operation can be seen above each task T1, whereas the number of passengers aboard the EB can be seen above each task T2. The initials inside the bars represent Magangué, Tanqueo, or Pinillos. The vertical dashed lines divide each pair of days. It can be seen in the graph that the EB always charges in Tanqueo during the outward trip. Thus, the EB always arrives at Pinillos with its minimum energy level and is therefore required to recharge. This forces the EB to always depart with just one passenger, following the en-route charging strategy. It can also be seen that the charging operations during the outward trip of each day's second round trip are quite substantial. This is because the previous charging operation in Magangué is always interrupted for the second round trip to start on time, forcing the EB to depart with less energy than desired. As previously mentioned, this schedule makes the daily operation of the EB rather tight timewise, which helps explaining the selected charging powers of the PVCSs and the speeds of the EB. It can also be seen that the interday charging operations are the main reasons why the EB charges more energy in Magangué on average, which, as mentioned before, helps explain such PVCS's greater ESS capacity.

Fig. 8 shows the daily energy usage of each PVCS for ten consecutive days to evaluate how the charging operations went. The values above each bar represent the number of charging operations performed on each station during a given day. The figure shows that most of the energy comes from the PV arrays and ESS, implying that it is possible to have an electric fluvial operation of this scale supplied mainly by PV energy. This situation helps explain significant investments in PV components. Additionally, it can be seen that the energy usage in Magangué and Pinillos is similar for all days, whereas that in Tanqueo varies significantly from day to day. The latter is due to differences in the EB's consumption given by the number of passengers transported during the outward trips. Days 1, 2, 3, 5, 6, and 9 transported an average of 7.5 passengers during the outward trips, whereas days 4, 7, 8, and 10 transported an average of 4.87 passengers. This is not the case for Pinillos as, given by our charging strategy, the EB decided to charge enough energy to depart with only one passenger. As for Magangué, given that it only performs interday and interroute operations, the charging decisions at that node are given by the available time to charge, not by the consumption to the following station. Additionally, the energy to charge between days in Magangué is the same everyday as the EB always arrives with the minimum energy level on its battery from the last round trip. Therefore, the amount of energy charged at Magangué was rather constant.

6.4. Sensitivity analyses

After analyzing the base scenario of the case study, we present different sensitivity analyses in this subsection. Regarding the reliability of the FPTDP-EB, one interesting analysis involves evaluating how the solution changes if the minimum required number of feasible days α increases. For doing so, Fig. 9 shows how the costs of the solution change as α increases. Each bar represents a different piece of the cost, such as the cost of the EB's battery, the components of the PVCSs, or the energy to be purchased from the grid. Values above the bars represent the rounded total cost of each solution. The lower part of the graph shows the number of installed stations and the selected capacity of the EB's battery. The scenario with $\alpha = 90\%$ is the one from the case study, whereas the one with 96% is the last scenario in which a feasible

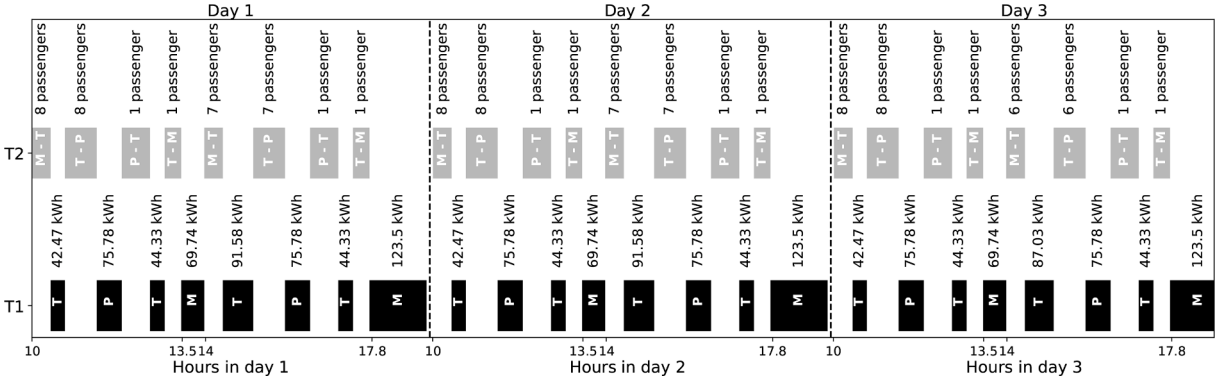

Fig. 7. The EB's daily operation.

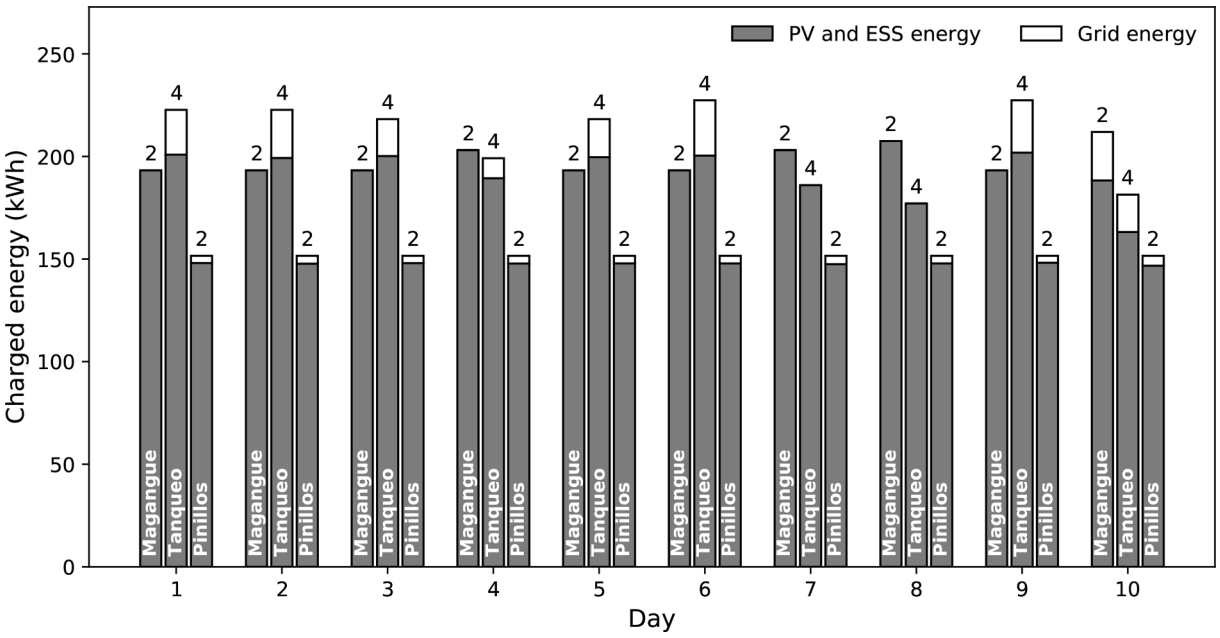

Fig. 8. Daily energy taken from the grid versus that taken from the PV arrays and ESS of each PVCS.

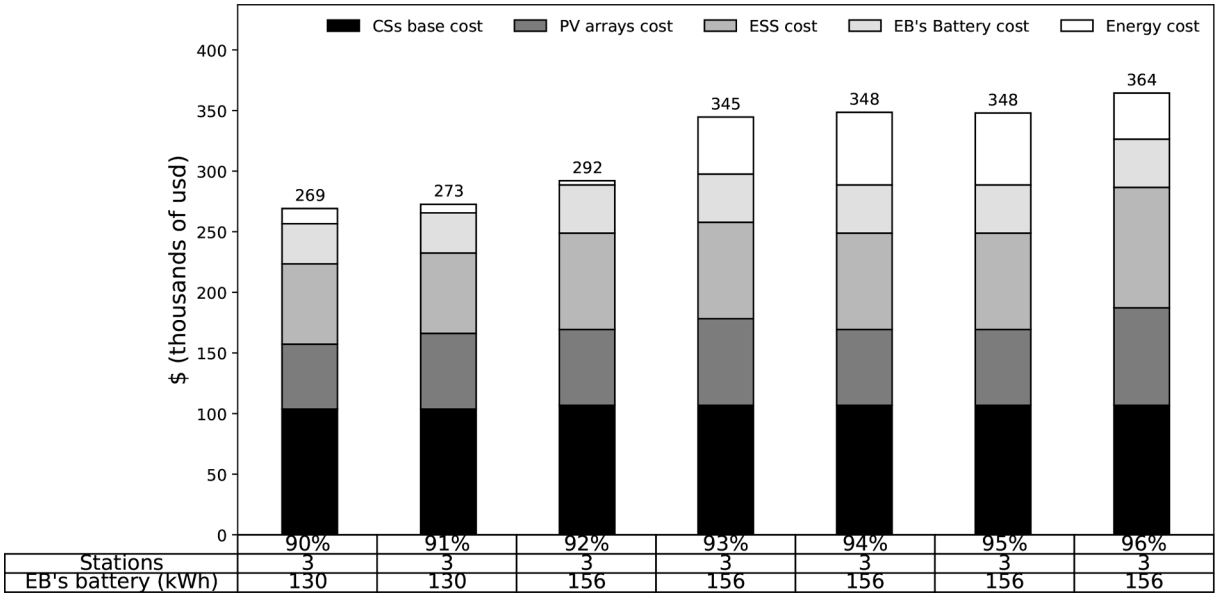

Fig. 9. Total costs with varying minimum percentages of days that must be feasible per replication.

solution was found. The latter scenario costs 35.34% more than the former. It can be seen that from the scenario with $\alpha \geq 92\%$, a larger battery capacity for the EB was required for the operation to be feasible. The most significant leap in costs was between the scenarios with $\alpha = 92\%$ and 93%. Such difference is primarily due to an increase in the amount of energy to be purchased from the grid. Such energy was required because the operation needed one additional round trip per day to meet service quality constraints for enough days. The main difference between the scenario with $\alpha = 93\%$ and either 94% or 95% is that for the first one, the speed during the return trip was 40 km/h rather than 50 km/h. This reduced the energy consumption and, therefore, the energy to be purchased from the grid. Consequently, it can be seen that asking for a more reliable operation requires a heavier investment and that such operation cannot be guaranteed to be feasible 100% of the time.

To measure the impact of the PVCSs, we evaluated a scenario where only SCSs were considered. To do so, we first tried setting the cost of the PV panels and DC-DC converters to over billions of USD each to heavily punish the use of PVCSs. However, while the solution for that scenario did install SCSs in the nodes in Magangué and Pinillos, it also installed a PVCS in Tanqueo. This means that there are no feasible solutions for the base scenario using only SCSs, which is due to the power outages. These outages also explain why the PVCS was installed in Tanqueo, as it is the station where most charging operations take place, therefore being the most likely one to suffer power outages. To fully compare the base scenario with one having no PVCSs, we effectively disable the power outages by considering a PDF with a mean value of over billions of years to generate the times between outages, and a PDF with mean value of 0 h for their duration. Table 7 shows the solution for this scenario, following the same structure as Table 5. As expected, the cost of the stations

decreased by 53.61% when compared to the base scenario, due to the absence of PV components. We note that the 1 C charging power was selected for all the SCSs. On the other hand, the amount of energy to purchase from the grid, and its cost, increased by 1658.96% and 1667.3%, respectively. We note that these percentages are not exactly equal to each other as the cost of energy from the grid varies between years in the simulation. Looking at the overall cost, the one for the solution using only SCSs increased by 33.01% when compared to the base scenario.

For the base scenario, we considered the battery energy density of 0.18 kWh/kg from ENERGETICA 2030's battery. However, battery energy densities tend to improve as time goes on, and according to Volkswagen (2018), they would be around 0.35 kWh/kg by 2030. Therefore, we performed two different sensitivity analyses to assess the changes in the total cost of the operation as such energy density increases. For doing so, we evaluated the following densities in kWh/kg: {0.18, 0.21, 0.25, 0.28, 0.32, 0.35}. The first value is the density of the current battery, and the last one is the estimated density by 2030. A change in the battery energy density can be analyzed from two different perspectives: maintaining the battery's capacity and reducing its weight or maintaining its weight and increasing its capacity. We evaluated both of these perspectives while keeping the battery's cost per kWh of 254.81 USD/kWh for both the EB's battery and the ESSs.

Fig. 10 shows how the total cost of the operation changes as the battery energy density increases for both of the aforementioned perspectives. Both figures follow a similar structure to that of Fig. 9. Fig. 10 (a) shows the analysis where the battery weight is decreased with constant battery capacity. Considering lower battery weights reduces the energy consumption of the EB, which in turn reduces the amount of energy to be purchased from the grid or the number of installed stations. There is a big leap in costs between the scenarios with densities of 0.21 and 0.25 kWh/kg. This is because the latter scenario installed one fewer station, which greatly reduced the total cost even at the expense of installing a larger battery capacity for the EB. There is another leap in cost between the scenarios with densities of 0.28 and 0.32 kWh/kg due to a lower battery capacity for the EB while maintaining the number of installed stations. The reduction in the total cost between the base scenario and the scenario with a 0.35-kWh/kg density was 34.3%. Fig. 10 (b) shows the results for the analysis where the battery capacity was increased with constant weight. Doing so helps decrease the number of installed stations. In this case, there is already a reduction in the number of installed stations between the 0.18- and 0.21-kWh/kg scenarios, with another one between the 0.25- and 0.28-kWh/kg scenarios. It can also be seen that the solution for the scenario with the density of 0.32 kWh/kg was actually more expensive than that with the density of 0.28 kWh/kg. This is because the overall cost of batteries increases with every scenario (as the cost per kWh was kept constant while the capacities increased). Therefore, having an analogous solution for two scenarios is more expensive with greater battery energy density because of the battery capacity. The solution method did not find a lower battery capacity for the EBs for the 0.32-kWh/kg scenario that would allow only one station to be installed, as in the 0.28-kWh/kg scenario. The reduction in the total cost between the base scenario and that with the 0.35-kWh/kg density was 34.6%. Both of these analyses show that as battery energy densities improve, the costs of this type of electric fluvial operations are expected to decrease greatly.

Table 7
General attributes of the solution using only SCSs.

Attribute of the solution	Value
Battery capacity of the EB (b)	130 kWh
Stations installed	3
Speed during the outward trip (s_o)	50 km/h
Speed during the return trip (s_r)	50 km/h
Departure hours (h)	10:00 and 14:00
Energy to purchase from the grid	1,621,922.29 kWh
Total cost	357,966.71 USD
Cost of the EB's battery (d_b^{BAT})	33,125.35 USD
Cost of the stations (including their maintenance)	103,663.18 USD
Cost of the energy to purchase from the grid	221,178.18 USD

As previously mentioned, rural areas may have reliability issues with the electric power grid, which was one of the reasons why we considered PVCSs in our research. Because of that, we wanted to evaluate how the solution may be affected if this reliability issue persisted. Fig. 11 shows how the costs of the solution would change if the average time between outages decreases and their average duration increases. Both factors were varied simultaneously and by the same factors, which can be seen below each bar. The differences in costs were not as significant as with the other previous analyses, with an increment of just 3.89% between the base scenario and the one in which the average time between outages decreased by a factor of 2 and their average duration increased by the same factor. Therefore, not enough power outages coincided with the EB's charging schedule to significantly affect the solution. The most significant increases in investment costs happened between scenarios with factors of 1 and 1.1 and between 1.4 and 1.5 and were due to slightly more significant investments in PV arrays. These changes in the time between power outages and their duration slightly decreased the overall use of energy from the grid, as shown, for example, in the slight difference in the rounded total costs of scenarios with factors of 1.3 and 1.4. These results indicate that even though we decreased the grid's reliability, feasible solutions can still be found and that their costs are not greatly affected. This is because most of the outages do not occur while the EB is charging, unlike what would happen for operations requiring a constant power supply from an external source, where these outages may have a more significant impact.

As the solution of the case study made some heavy investments in PVCSs, we wanted to evaluate a pessimistic scenario in terms of solar irradiance to assess how it would affect the results. For doing so, we considered the daily average irradiance values for 20 years' worth of data from NSRDB (2022) and selected the days for which such averages were lower outliers. There were 164 such days in total. Then, we made it so that for each day of each replication, the algorithm randomly selected one of those 164 days from which to source its solar irradiance data. Tables 8 and 9 show the solution of such scenario following the same structure of Tables 5 and 6. Table 9 shows that the overall cost increased by 19.92% when compared with that of the base scenario. This is because the amount of energy purchased from the grid increased by about 414.68%, costing 64,844.46 USD. Table 9 shows that the increment in energy to purchase from the grid occurred even though more PV arrays were installed in Tanqueo and Pinillos. Additionally, the capacity of the ESS of Magangué's PVCS was decreased as the PV generation was not enough to make it worth installing the 130-kWh ESS. However, this smaller ESS almost compensated the extra monetary investment in PV arrays, as the investment costs of this pessimistic scenario were only 0.5% greater than those of the base one. Finally, we note that even for this pessimistic scenario, all installed stations were PVCSs rather than SCSs.

7. Insights

In this research we studied the specific case study of the alliance "ENERGETICA 2030". However, we believe that this work can be applicable in other regions that are aiming to implement electric fluvial transport operations. Because of that, in this section we provide some insights that may help policy makers in future implementations this type of transport operations.

- The results of the case study show that most of the total cost of the solution came from the stations. Such stations were needed due to the demanding requirements of the operation in terms of route length and time. Because of that, we recommend future electric fluvial transport operation to be implemented in less demanding

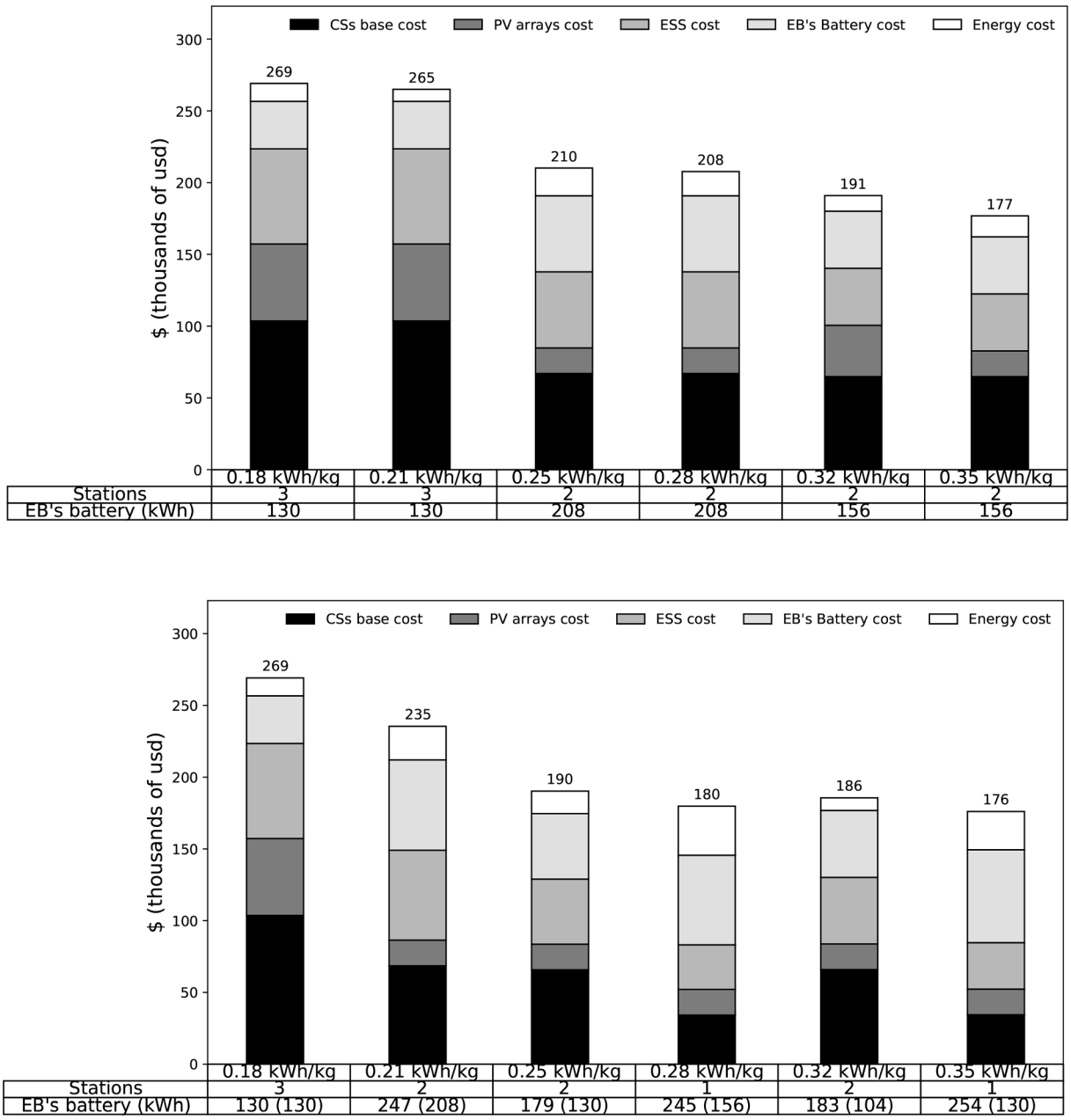

Fig. 10. Changes in the total costs of the operation as the battery energy density increases.

contexts to reduce costs. We propose considering shorter routes where fewer stations are required, or having more available time for charging operations so that lower charging powers are selected for the stations. In either case, we suggest using optimization models to minimize the costs of the operations.

- One of the most impactful parameters in our case study is the energy density of the EB's battery. However, as we mentioned before, the densities of these batteries have been improving with the years and are expected to continue doing so. In that regard, our sensitivity analyses show that such improvements would considerably decrease the costs of electric fluvial transport operations in the future.
- At the time of this writing, most the charging stations do not have PV system as they are targeted for urban areas where the electric grid is stable enough. However, as mentioned before, fluvial transport operations tend to be implemented in rural areas where power outages are common. PVCSs are more suited than SCSs for these types of regions as they do not rely entirely on the electric grid, as shown by our result where no feasible solution was found using only SCSs. Additionally, our results show that using PVCSs can help minimizing the total cost of this type of operations over the years.

The previous insights are outcomes of our results. However, we additionally want to make a general reflection for future policy makers regarding the potential of electric fluvial transport operations for resilient transport systems. Not only are these operations crucial in regions where land transport is infeasible, but they are also a viable way of transportation in cities that suffer from floods (Åkeson and Salzenstein, 2021). On top of that, the use of EBs in such cities can provide a sustainable and economical alternative to oversaturated public transport systems (Campillo et al., 2019).

8. Conclusions and future work

In this research, we introduced a new optimization problem called

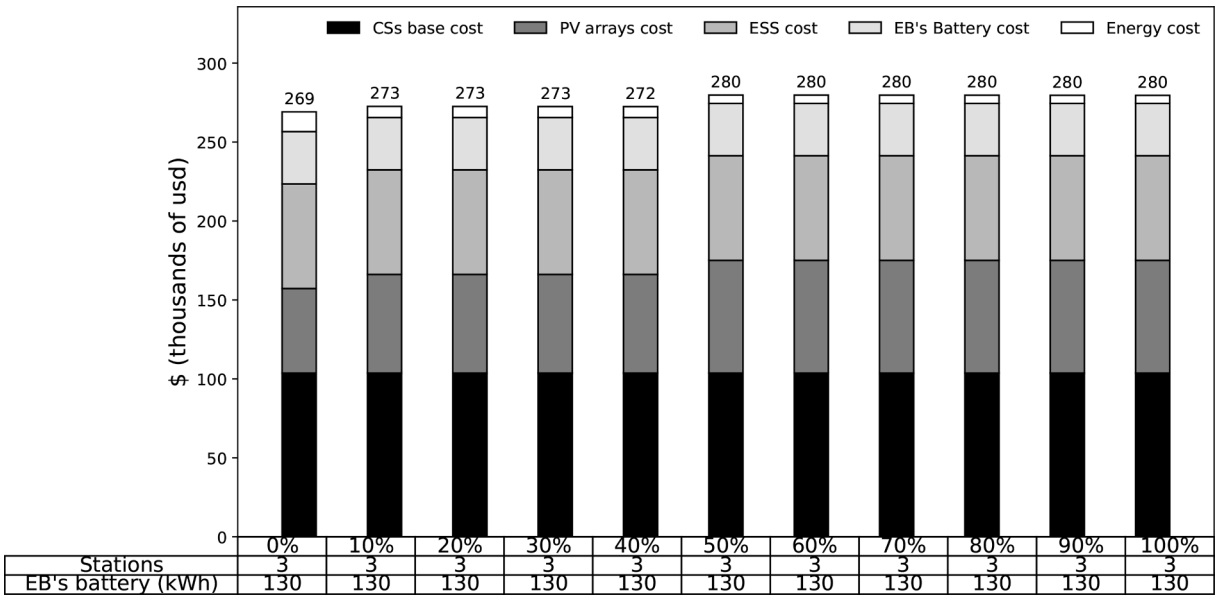

Fig. 11. Total costs with varying average times between outages and their average duration.

Table 8
General attributes of the solution of the scenario with low solar irradiance.

Attribute of the solution	Value
Battery capacity of the EB (b)	130 kWh
Stations installed	3
Speed during the outward trip (s_o)	50 km/h
Speed during the return trip (s_r)	50 km/h
Departure hours (h)	10:00 and 14:00
Energy to purchase from the grid	475,507.9 kWh
Total cost	322,746.7 USD
Cost of the EB's battery (d_b^{BAT})	33,125.35 USD
Cost of the stations (including their maintenance)	224,776.89 USD
Cost of the energy to purchase from the grid	64,844.46 USD

Table 9
PCVS related attributes of the solution of the scenario with low solar irradiance.

Attribute of the solution	Magangué	Tanqueo	Pinillos
Number of PV arrays (arrays)	14	21	21
ESS capacity (% of b)	50	50	50
Charging power (C rate)	1 C	1 C	1 C

the FPTDP-EB. The problem consists of selecting the battery capacity for the EB, the charging infrastructure to install, the average speeds of the EB during the outward and return trips, and the departure times of the round trips to be performed. The objective function is to minimize the investment costs given by the EB's battery and the charging infrastructure, the maintenance cost of the charging stations and the energy to be purchased from the grid for a set of years of the EB's operation. This problem is inspired by the need to design a future fluvial transport operation using EBs in Magangué, Colombia. We proposed a simulated-base branch-and-bound algorithm to solve this problem and, therefore, the case study. Despite all the constraints that a rural operation with an EB faces, such as the limited autonomy of the EB, and dealing with power outages, the method found a feasible solution for the case study. The main characteristic of the solution is that using PVCSs helps decrease the overall operational cost. This is because even though 83.04% of the total investment was in PVCSs, the amount of energy from the grid that they help save compensate for it. Additionally, the solution installed a PVCS in every single node because of the limited energy density of the EB's battery.

On the basis of the case study's scenarios, we performed some sensitivity analyses by varying some key aspects of the problem. The first aspect that we evaluated was increasing the minimum percentage of feasible days required per replication of the simulation, α, as this is related to the reliability of the design. We found that for $\alpha \leqslant 96\%$, feasible solutions to the problem were found, which shows that the design may be highly reliable. However, higher values of α require higher investments, as expected. The second aspect that we evaluated was having a solution with only SCSs. We found that, due to the power outages, there is no feasible solution to our case study using only SCSs. We then disable the power outages, and found that using only SCSs increases the overall cost of the solution by 33.01%. The third aspect that we varied was the battery energy density, which has been improving over time and is expected to continue doing so. Our analyses showed that improving the battery energy densities significantly decreases the overall design cost, with cost reductions of around 34% for an expected scenario by 2030. This reduction was mostly because fewer PVCSs were needed. The fourth aspect we varied was the electric grid's reliability, which may be crucial in rural areas. For doing so, we decreased the average time between outages and increased their average duration. Our analysis showed that feasible solutions to the problem could still be found and that their cost did not change significantly, even for a scenario where both average values were varied by a factor of 2. The last analysis we performed was considering a scenario with low solar irradiance, which we evaluated as the solution to the problem was installing PVCSs. Therefore, we wanted to assess the impact of having lower solar irradiance. The analysis showed that feasible solutions could still be found and that their costs were significantly increased, which was primarily because the amount ofenergy to be purchased from the grid also increased. These sensitivity analyses showed that implementing reliable electric fluvial transport operations in rural areas is feasible and that their costs are expected to significantly decrease as battery energy densities increase.

Some interesting directions for future researches include considering scenarios with multiple EBs or even different types of EVs sharing some of the charging infrastructure. Considering multiple EBs would most certainly required changing the infrastructure decisions, while likely making the scheduling decisions of each EB less tight timewise. The second scenario could include some charging stations being shared by EBs and electric cars owned by a certain transport company in port cities. This scenario could raise some questions such as how to

coordinate the charging of each type of vehicle to optimize the use of photovoltaic energy.

Financial Disclosure: none.

CRediT authorship contribution statement

Camilo Vélez: Formal analysis, Investigation, Methodology, Software, Data curation, Writing – original draft, Visualization. **Alejandro Montoya:** Conceptualization, Investigation, Formal analysis, Methodology, Data curation, Supervision, Writing – review & editing.

Declaration of Competing Interest

The authors declare that they have no known competing financial interests or personal relationships that could have appeared to influence the work reported in this paper.

Acknowledgements

The authors would like to thank Universidad EAFIT and the alliance ENERGETICA 2030, which is a Research Program with code 58667 from the Colombia Científica initiative, funded by The World Bank through the call 778-2017 Scientific Ecosystems. The research program is managed by the Colombian Ministry of Science, Technology and Innovation (Minciencias) with contract No. FP44842-210-2018. Additionally, the authors would like to acknowledge the supercomputing resources made available by the Centro de Computación Científica APOLO at Universidad EAFIT (www.eafit.edu.co/apolo) to conduct the research reported in this paper.

References

AFDC, 2018. Electric vehicle charger selection guide.https://afdc.energy.gov/files/u/publication/EV_Charger_Selection_Guide_2018-01-112.pdf, Accessed October 2022.

Afinia, 2022. Tarifas y Subsidios.https://energiacaribemar.co/tu-energia/, Accessed October 2022.

Agrawal, A., 2018. Modeling forced outage in hydropower generating units for operations planning model (Ph.D. thesis). University of British Columbia.

Åkeson, J., Salzenstein, L., 2021. Climate change adaptation and urban development: a genealogy of flood risk management in Glasgow (Master's thesis). Lund University.

Alvarado Ponce, L., 2017. Estudio del potencial de las embarcaciones solares en la Amazonía: caso de estudio Río Napo (Ph.D. thesis). ETSI_Diseno.

Baek, D., Chen, Y., Chang, N., Macii, E., Poncino, M., 2020. Optimal battery sizing for electric truck delivery. Energies 13, 709.

Battery University, 2017. Bu-402: What is c-rate? https://batteryuniversity.com/learn/article/what_is_the_c_rate, Accessed October 2022.

Bhatti, A.R., Salam, Z., Aziz, M.J.B.A., Yee, K.P., Ashique, R.H., 2016. Electric vehicles charging using photovoltaic: Status and technological review. Renew. Sustain. Energy Rev. 54, 34–47.

Bloomberg, 2019. Electric car price tag shrinks along with battery cost. <https://www.bloomberg.com/opinion/articles/2019-04-12/electric-vehicle-battery-shrinks-and-so-does-the-total-cost>, Accessed October 2022.

Bloomberg, 2021. China cracks the trillion-dollar ev question. https://www.bloomberg.com/opinion/articles/2021-04-15/biden-s-ev-infrastructure-plan-should-take-a-page-from-china/, Accessed October 2022.

Campillo, J., Domínguez-Jimenez, J., Cabrera, J., 2019. Sustainable boat transportation throughout electrification of propulsion systems: Challenges and opportunities, in: 2019 2nd Latin American Conference on Intelligent Transportation Systems (ITS LATAM), pp. 1–6. DOI: 10.1109/ITSLATAM.2019.8721330.

Cao, W., Zhang, J., Li, H., 2020. Batteries with high theoretical energy densities. Energy Storage Mater. 26, 46–55.

Chen, T., Zhang, X.P., Wang, J., Li, J., Wu, C., Hu, M., Bian, H., 2020. A review on electric vehicle charging infrastructure development in the uk. J. Modern Power Syst. Clean Energy 8, 193–205.

Cristaldi, L., Faifer, M., Rossi, M., Toscani, S., 2012. Mppt definition and validation: A new model-based approach, in: 2012 IEEE International Instrumentation and Measurement Technology Conference Proceedings, IEEE. pp. 594–599.

Eccarius, T., Lu, C.C., 2020. Powered two-wheelers for sustainable mobility: A review of consumer adoption of electric motorcycles. Int. J. Sustain. Transp. 14, 215–231.

Energetica 2030, n.d. Colombia Científica. https://www.energetica2030.co/ Accessed October 2022.

Espinouse, M., Lacomme, P., Moukrim, A., Tchernev, N., 2000. Branch and bound approach based on simulation for the job input sequencing and device dispatching in fms. IFAC Proceedings Volumes 33, 729–734.

Galadima, A.A., Zarma, T.A., Aminu, M.A., 2019. Review on optimal siting of electric vehicle charging infrastructure. J. Scientific Res. Rep. 25, 1–10.

Gómez, A., Mariño, R., Akhavan-Tabatabaei, R., Medaglia, A.L., Mendoza, J.E., 2016. On modeling stochastic travel and service times in vehicle routing. Transp. Sci. 50, 627–641.

Hossain, M.A., Pota, H.R., Squartini, S., Zaman, F., Muttaqi, K.M., 2019. Energy management of community microgrids considering degradation cost of battery. J. Energy Storage 22, 257–269.

Hu, Q., Zhang, Z., Lim, A., 2016. Transportation service procurement problem with transit time. Transp. Res. Part B: Methodol. 86, 19–36.

Insider, 2021. Amazon's first electric delivery vans are now making deliveries – see how they were designed. https://www.businessinsider.com/amazon-creating-fleet-of-electric-delivery-vehicles-rivian-2020-2/, Accessed October 2022.

International Energy Agency, 2021. Global ev outlook 2021. https://www.iea.org/reports/global-ev-outlook-2021/trends-and-developments-in-electric-vehicle-markets, Accessed October 2022.

Jaimurzina, A., Wilmsmeier, G., Montiel, D., 2017. Eficiencia energética y movilidad eléctrica fluvial: soluciones sostenibles para la Amazonía. CEPAL.

Krupp, C., 2010. Electrifying rural areas: extending electricity infrastructure and services in developing countries. In: Physical Infrastructure Development: Balancing the Growth, Equity, and Environmental Imperatives. Springer, pp. 203–224.

Lukuyu, J., Muhebwa, A., Taneja, J., 2020. Fish and chips: Converting fishing boats for electric mobility to serve as minigrid anchor loads, in: Proceedings of the Eleventh ACM International Conference on Future Energy Systems, pp. 208–219.

Macellari, M., Grasselli, U., Capponi, F.G., Schirone, L., 2013. Series-connected converters with individual mppt for bipv, in: 2013 International Conference on Clean Electrical Power (ICCEP), IEEE. pp. 52–56.

Minami, S., Yamachika, N., 2004. A practical theory of the performance of low velocity boat. J. Asian Electric Vehicles 2, 535–539.

MinHacienda, 2017. Marco fiscal de mediano plazo 2017. https://www.minhacienda.gov.co/webcenter/portal/EntidadesFinancieras/pages_EntidadesFinancieras/marcofiscalmedianoplazo/marcofiscaldemedianoplazo2017, Accessed October 2022.

Mobility Foresights, 2021. Global electric boat market. https://mobilityforesights.com/product/electric-boat-market/, Accessed October 2022.

Molland, A.F., Turnock, S.R., Hudson, D.A., 2017. Ship resistance and propulsion. Cambridge University Press.

Montoya, A., Guéreta, C., Mendoza, J.E., Villegas, J.G., 2017. The electric vehicle routing problem with non linear charging function. Transp. Res. Part B 103, 87–110.

Morrison, D.R., Jacobson, S.H., Sauppe, J.J., Sewell, E.C., 2016. Branch-and-bound algorithms: A survey of recent advances in searching, branching, and pruning. Discrete Optim. 19, 79–102.

NASA, 2008. Solar irradiance. https://www.nasa.gov/mission_pages/sdo/science/solar-irradiance.html, Accessed October 2022.

Nicholas, M., 2019. Estimating electric vehicle charging infrastructure costs across major u.s. metropolitan areas. https://theicct.org/sites/default/files/publications/ICCT_EVeCharging_Cost_20190813.pdf, Working paper, Accessed October 2022.

NSRDB, n.d. Nsrdb data viewer. https://maps.nrel.gov/nsrdb-viewer/ Accessed October 2022.

Ostadi, A., Kazerani, M., 2014. A comparative analysis of optimal sizing of battery-only, ultracapacitor-only, and battery–ultracapacitor hybrid energy storage systems for a city bus. IEEE Trans. Veh. Technol. 64, 4449–4460.

Oyola, J., Arntzen, H., Woodruff, D.L., 2018. The stochastic vehicle routing problem, a literature review, part i: models. EURO J. Transp. Logist. 7, 193–221.

Pelletier, S., Jabali, O., Mendoza, J.E., Laporte, G., 2019. The electric bus fleet transition problem. Transp. Res. Part C 109, 174–193.

Portafolio, 2018. El impuesto al carbono: tiempo de cambios. https://www.portafolio.co/opinion/luis-augusto-yepes/el-impuesto-al-carbono-tiempo-de-cambios-analisis-524116, Accessed October 2022.

Quddus, M.A., Kabli, M., Marufuzzaman, M., 2019. Modeling electric vehicle charging station expansion with an integration of renewable energy and vehicle-to-grid sources. Transp. Res. Part E 128, 251–279.

Ramakrishna, R., Scaglione, A., 2016. A compressive sensing framework for the analysis of solar photo-voltaic power. In: 2016 50th Asilomar Conference on Signals, Systems and Computers. IEEE, pp. 308–312.

Research and Markets, 2021. China's electric two-wheeler growth opportunities. https://www.researchandmarkets.com/reports/5411873/chinas-electric-two-wheeler-growth-opportunities, Accessed October 2022.

Savitsky, D., 1964. Hydrodynamic design of planing hulls. Marine Technology and SNAME News 1, 71–95.

Shepero, M., Lingfors, D., Widén, J., Bright, J.M., Munkhammar, J., 2020. Estimating the spatiotemporal potential of self-consuming photovoltaic energy to charge electric vehicles in rural and urban nordic areas. J. Renew. Sustain. Energy 12, 046301.

Solartex, 2020. Controlador MPPT 60A ML4860 12/24/48 SRNE. https://www.solartex.co/tienda/producto/controlador-de-carga-solar-ml4860/, Accessed October 2022.

Solartex, 2020. Panel solar 465 Watts Jinko TIGER Mono. https://www.solartex.co/tienda/producto/panel-solar-465-watts-jinko-tiger-mono/, Accessed October 2022.

Song, Z., Li, J., Han, X., Xu, L., Lu, L., Ouyang, M., Hofmann, H., 2014. Multi-objective optimization of a semi-active battery/supercapacitor energy storage system for electric vehicles. Appl. Energy 135, 212–224.

Soto, C., Dorronsoro, B., Fraire, H., Cruz-Reyes, L., Gomez-Santillan, C., Rangel, N., 2020. Solving the multi-objective flexible job shop scheduling problem with a novel parallel branch and bound algorithm. Swarm Evol. Comput. 53, 100632.

Sun, Z., Gao, W., Li, B., Wang, L., 2018. Locating charging stations for electric vehicles. Transport Policy 98, 48–54.

Superservicios, 2017. Diagnóstico de la calidad del servicio de energía eléctrica en colombia 2016. https://www.superservicios.gov.co/sites/default/files/inline-files/20170521_informeejecutivocalidaddelserviciofinal_1%20%281%29.pdf, Accessed October 2022.

Superservicios, 2019. Diagnóstico de la calidad del servicio de energía eléctrica en colombia en 2018. https://www.superservicios.gov.co/sites/default/files/inline-files/diagnostico_calidad_servicio_2018%20%281%29.pdf, Accessed October 2022.

The Guardian, 2020. Nasa leads push for electric planes in next frontier of cutting emissions. https://www.theguardian.com/us-news/2021/may/18/electric-planes-nasa-carbon-emissions, Accessed October 2022.

Umar, M., Ji, X., Kirikkaleli, D., Alola, A.A., 2021. The imperativeness of environmental quality in the united states transportation sector amidst biomass-fossil energy consumption and growth. J. Clean. Prod. 285, 124863.

UNEF, 2017. Kara solar, el primer sistema de transporte solar para la amazonía. https://www.unef.es/es/comunicacion/comunicacion-post/kara-solar-el-primer-sistema-de-transporte-solar-para-la-amazonia/, Accessed October 2022.

UPME, 2020. Cálculo del Factor de Emisión de Co2 del SIN. https://www1.upme.gov.co/siame/Paginas/calculo-factor-de-emision-de-Co2-del-SIN.aspx, Accessed October 2022.

U.S. Department of Energy, 2015. Costs associated with non-residential electric vehicle supply equipment. https://afdc.energy.gov/files/u/publication/evse_cost_report_2015.pdf Accessed October 2022.

U.S. Department of Transportation, 2019. Rural public transportation systems. https://www.transportation.gov/mission/health/Rural-Public-Transportation-Systems/ Accessed October 2022.

U.S. Department of Transportation, 2022. Rural opportunities to use transportation for economic success (routes). https://www.transportation.gov/rural Accessed October 2022.

Vélez, C., Villa, D., Montoya, A., 2020. Infrastructure estimation for a freight/personal transport operation with an electric boat on the magdalena river. Workshop on Engineering Applications, Springer 329–337.

Villa, D., Montoya, A., 2018. A taxonomy of energy consumption models for electric vehicles, in: OVICI-MOYCOT 2018: Joint Conference for Urban Mobility in the Smart City, IET.

Villa, D., Montoya, A., Ciro, J.M., 2019. The electric boat charging problem. Production 29.

Villa, D., Montoya, A., Herrera, A.M., 2020. The electric riverboat charging station location problem. Journal of Advanced Transportation 2020.

Volkswagen, 2018. Powerful and scalable. https://www.volkswagen-newsroom.com/en/stories/powerful-and-scalable-4244, Accessed October 2022.

Yan, D., Ma, C., 2020. Stochastic planning of electric vehicle charging station integrated with photovoltaic and battery systems. IET Gener. Transmission Distrib. 14, 4217–4224.

Zhang, L., Hu, X., Wang, Z., Sun, F., Deng, J., Dorrell, D.G., 2017a. Multiobjective optimal sizing of hybrid energy storage system for electric vehicles. IEEE Trans. Veh. Technol. 67, 1027–1035.

Zhang, W., Yan, X., Zhang, D., 2017b. Charging station location optimization of electric ship based on backup coverage model. TransNav, Int. J. Mar. Navigation Safety od Sea Transp. 11.